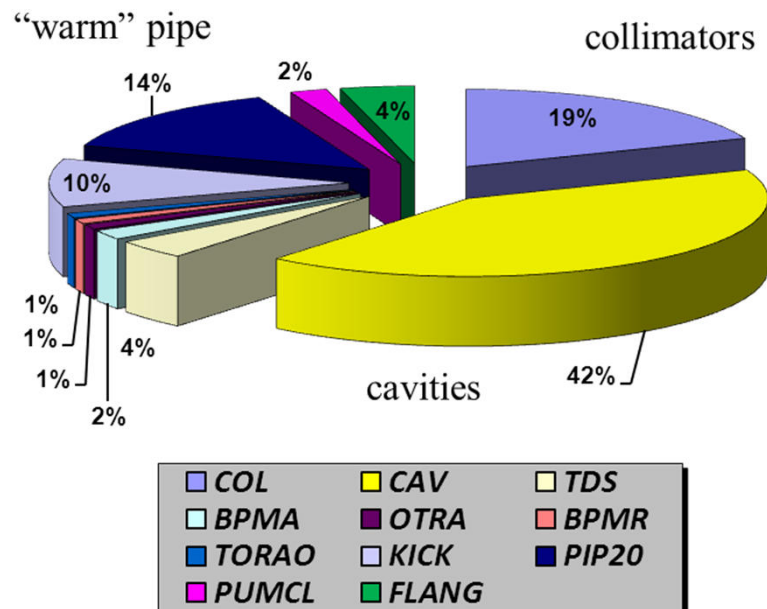


Wake Field Calculations at DESY

Impedance Budget for the European XFEL



Igor Zagorodnov

Collaboration Meeting at PAL

Pohang, Korea

2-6. September 2013

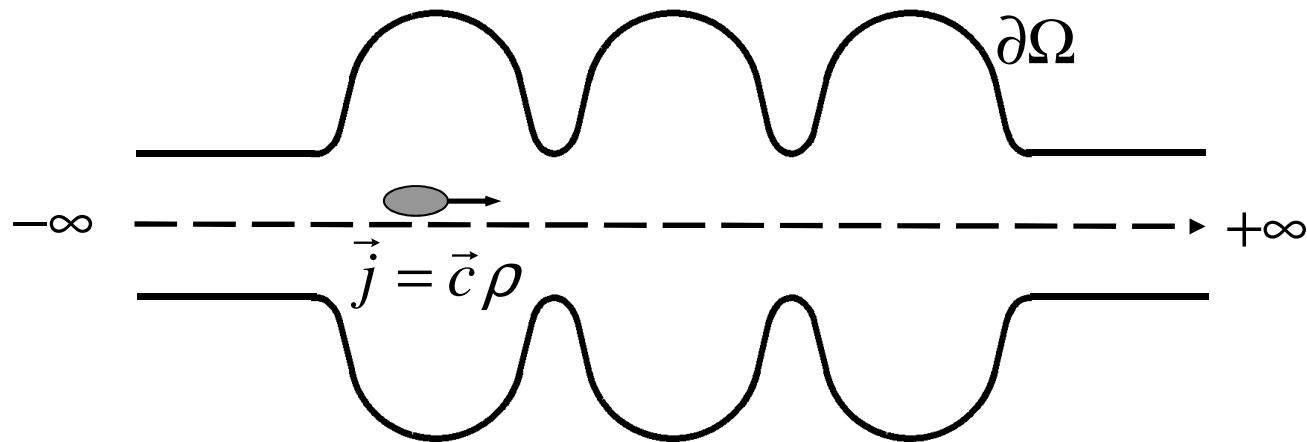
Overview

- ❑ Numerical Methods for Wake Field Calculations
 - ❑ low-dispersive schemes
 - ❑ indirect integration algorithm
 - ❑ modelling of conductive walls
 - ❑ optical approximation
 - ❑ slowly tapered transitions
- ❑ The European XFEL Impedance Budget
 - ❑ cavity and couplers wakes
 - ❑ collimator wakes
 - ❑ high-frequency impedances
 - ❑ longitudinal impedance budget



Low-dispersive schemes

Wake field calculation – estimation of the effect of the geometry variations on the bunch



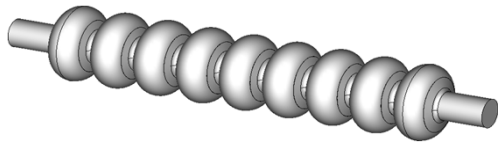
First codes in time domain ~ 1980

A. Novokhatski (BINP),

T. Weiland (CERN)

Low-dispersive schemes

TESLA cavity



Gaussian bunch with RMS length $\sigma = 50\mu\text{m}$

3 cryomodules to reach steady state
– about **36 m**

New projects – new needs

- short bunches;
- long structures;
- tapered collimators

New methods are required

- without dispersion error accumulation;
- “staircase” free;
- fast 3D calculations on PC

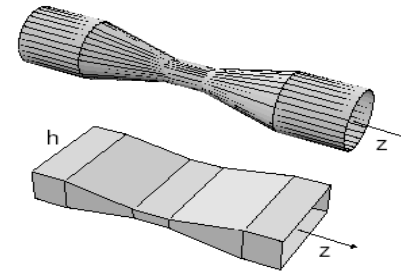
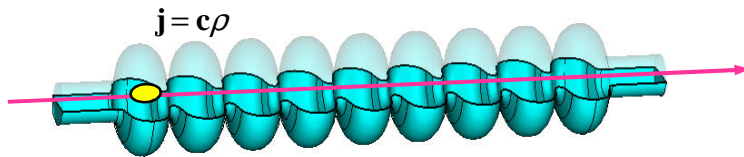


Solutions

- zero dispersion in longitudinal direction;
- “conformal” meshing;
- moving mesh and “explicit” or “split” methods



Low-dispersive schemes



Long smooth structures in **3D**

MAFIA, ABCI

E/M* scheme

- ☹ grid dispersion
- ☹ staircase geometry approximation
- ☹ moving mesh demands interpolation

ECHO-3D

TE/TM scheme**

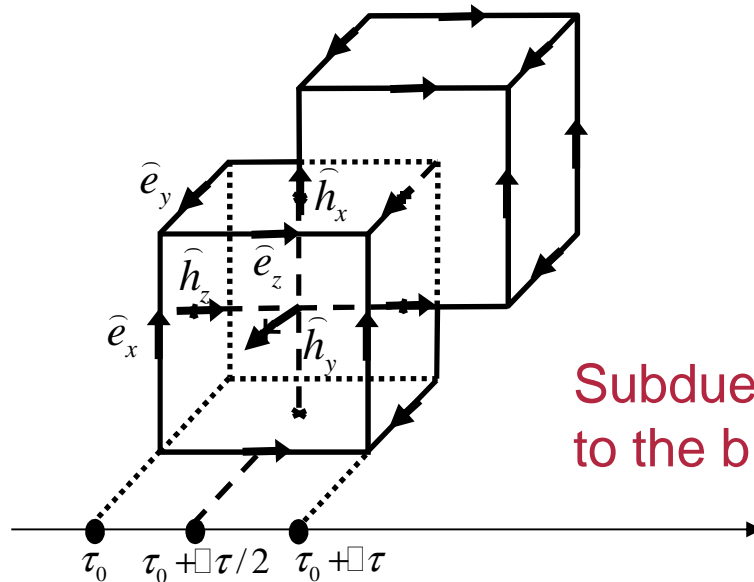
- ☺ zero dispersion in longitudinal direction.
- ☺ staircase free (second order convergent)
- ☺ travelling mesh easily (mesh step is equal to time step)

*E/M- „electric - magnetic“ splitting of the field components in time = Yee's FDTD scheme

**TE/TM- „transversal electric - transversal magnetic“ splitting of the field components in time

Low-dispersive schemes

E/M and TE/TM splitting



Subdue the updating procedure to the bunch motion

E/M splitting

TE/TM splitting

$$\mathbf{h}^n = \begin{pmatrix} \mathbf{h}_x^n \\ \mathbf{h}_y^n \\ \mathbf{h}_z^n \end{pmatrix} \quad \mathbf{e}^{n+0.5} = \begin{pmatrix} \mathbf{e}_x^{n+0.5} \\ \mathbf{e}_y^{n+0.5} \\ \mathbf{e}_z^{n+0.5} \end{pmatrix}$$

MAFIA

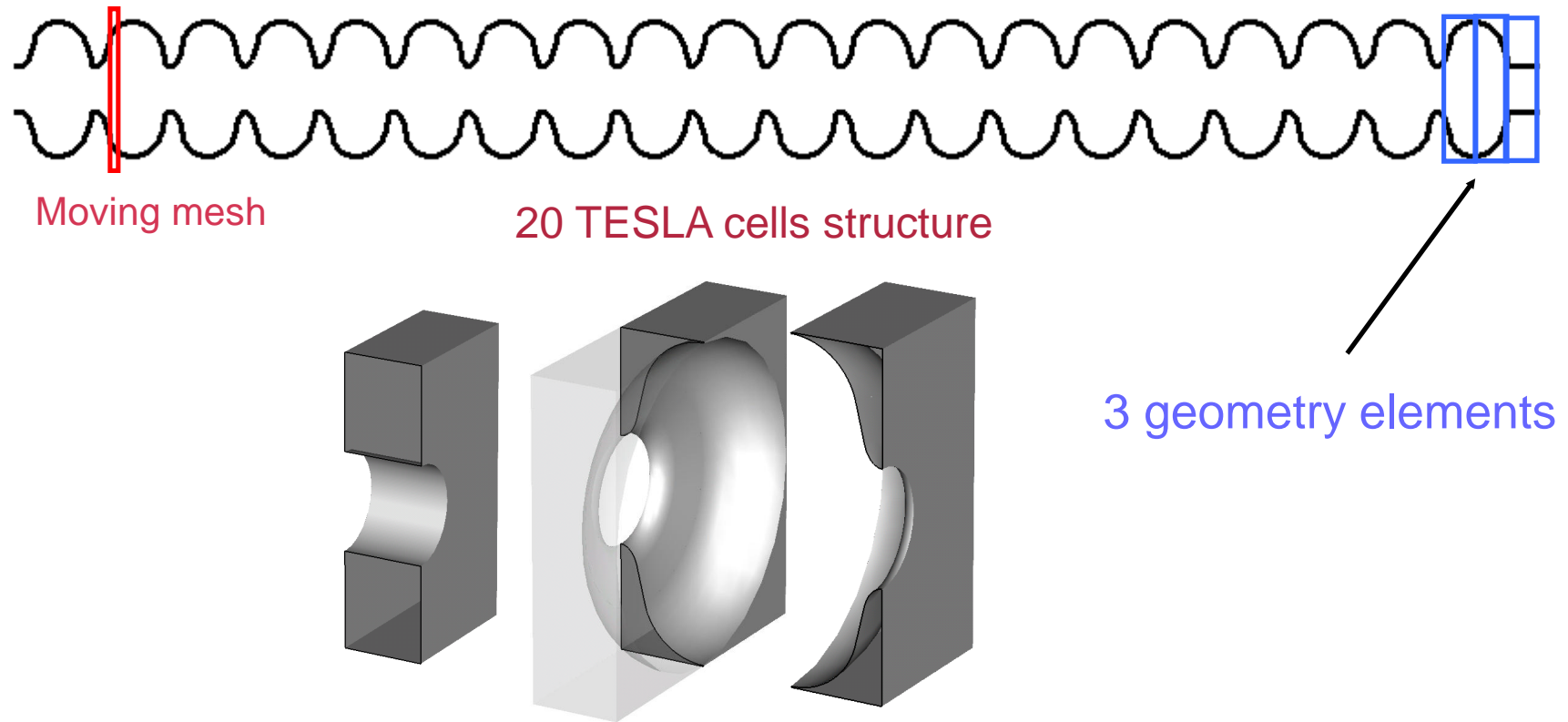
$$\mathbf{v}^n = \begin{pmatrix} \mathbf{e}_x^n \\ \mathbf{e}_y^n \\ \mathbf{h}_z^n \end{pmatrix} \quad \mathbf{u}^{n+0.5} = \begin{pmatrix} \mathbf{h}_x^{n+0.5} \\ \mathbf{h}_y^{n+0.5} \\ \mathbf{e}_z^{n+0.5} \end{pmatrix}$$

ECHO-3D



Low-dispersive schemes

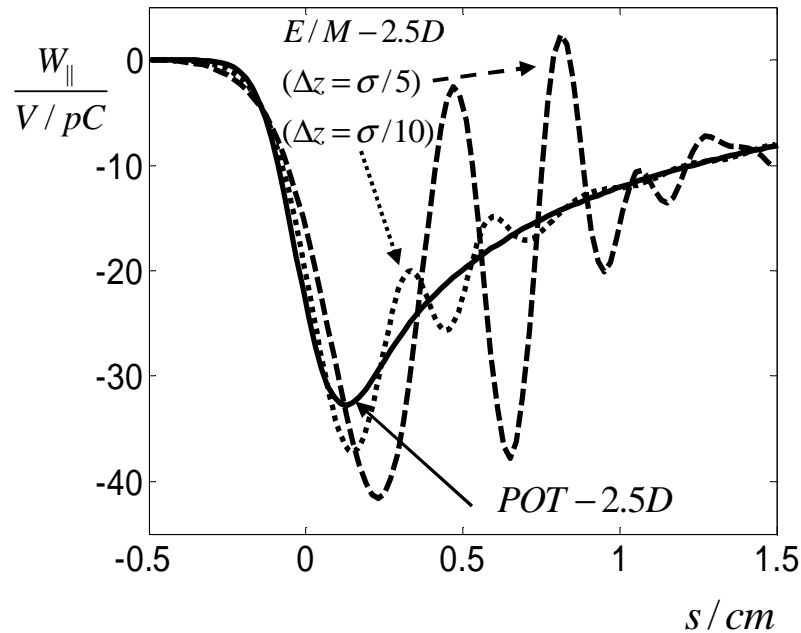
3D simulation. Test examples



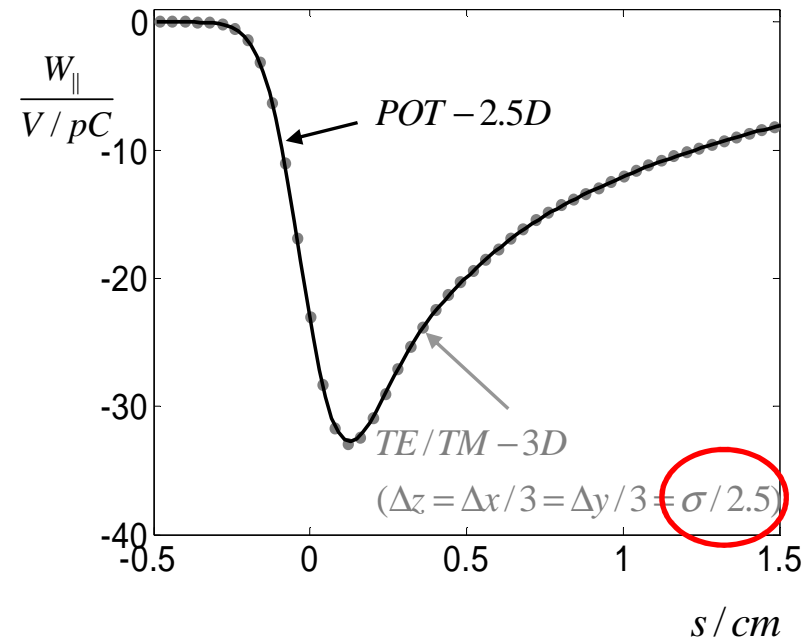
The geometric elements are loaded at the instant when the moving mesh reach them.
During the calculation only 2 geometric elements are in memory.

Low-dispersive schemes

MAFIA



ECHO-3D



Comparison of the wake potentials obtained by different methods for structure consisting of 20 TESLA cells excited by Gaussian bunch $\sigma = 1mm$

E/M splitting

$$\Delta z \sim \sqrt{\frac{\sigma^3}{L}}$$

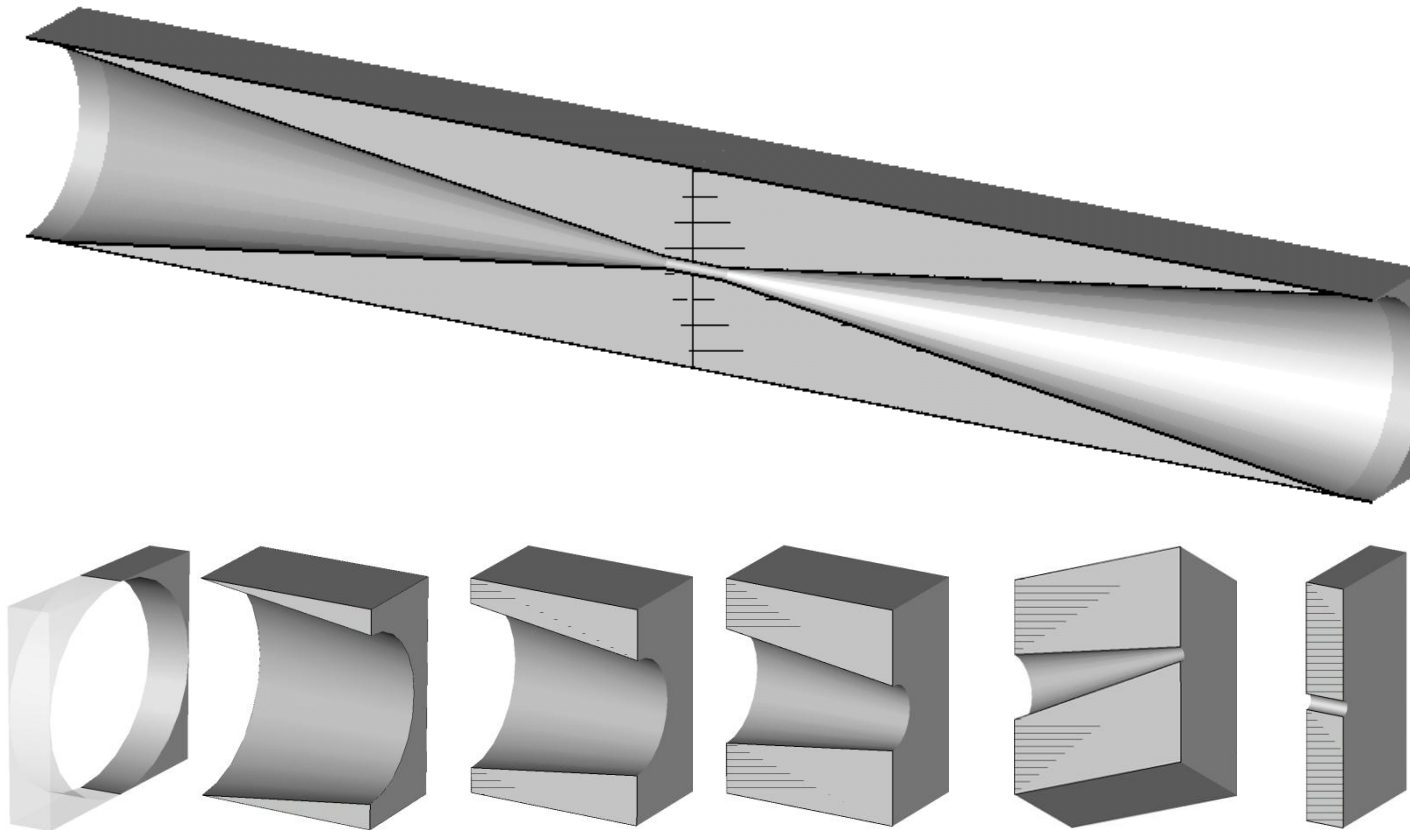
TE/TM splitting

$$\Delta z \sim \sigma$$

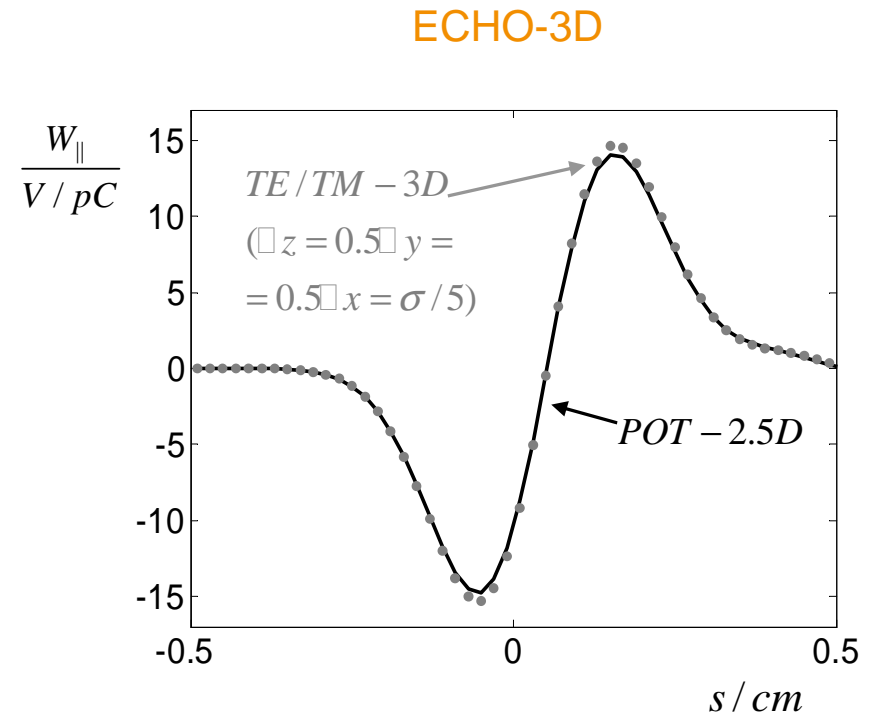
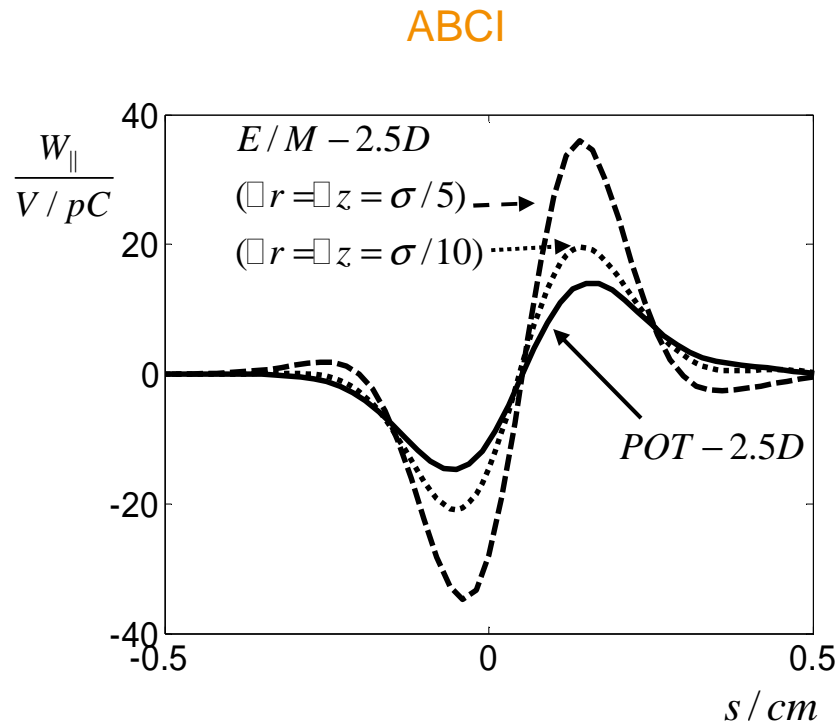


Low-dispersive schemes

3D simulation. Collimator



Low-dispersive schemes



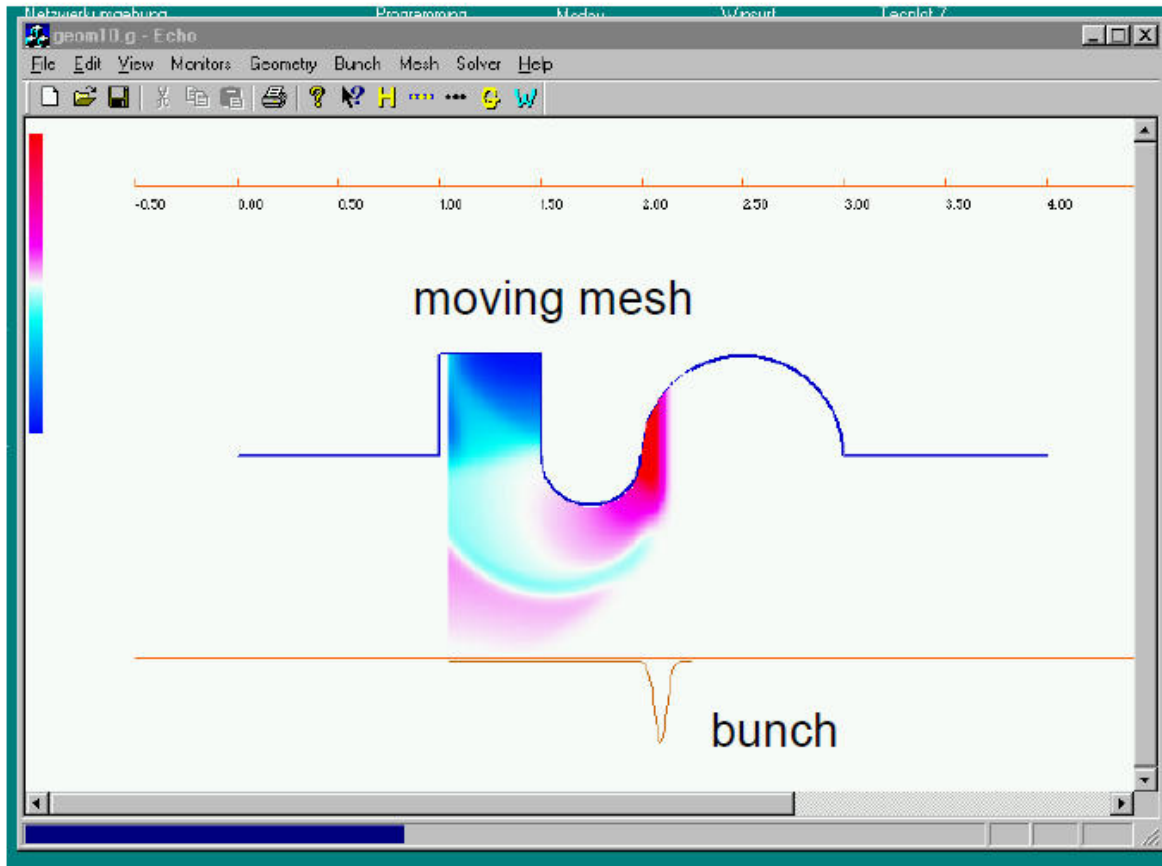
Comparison of the wake potentials obtained by different methods for round collimator excited by Gaussian bunch $\sigma = 1mm$

TE/TM method – fast, stable and accurate with coarse mesh

Zagorodnov I., Weiland T., *TE/TM Scheme for Computation of Electromagnetic Fields in Accelerators* // Journal of Computational Physics, **2004**.



Low-dispersive schemes

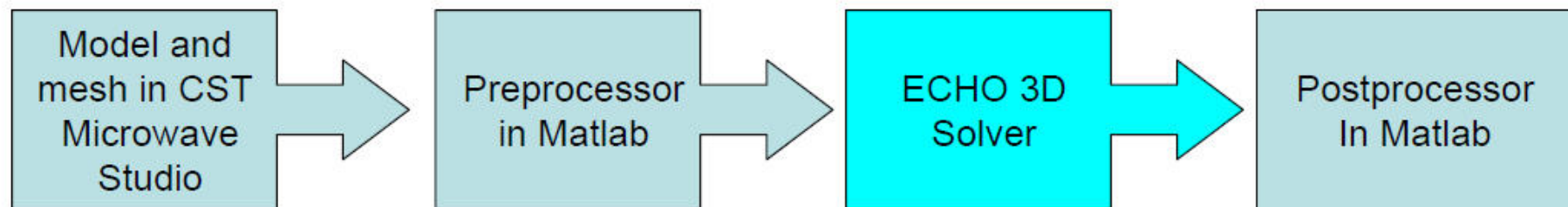


Electromagnetic
Code for
Handling
Of
Harmful
Collective
Effects

Zagorodnov I, Weiland T., *TE/TM Field Solver for Particle Beam Simulations without Numerical Cherenkov Radiation*// Physical Review – STAB,8, **2005**.

Low-dispersive schemes

- **zero dispersion** in z-direction
 - **staircase free** (second order convergent)
 - **moving mesh** without interpolation
 - in **2.5D** stand alone application
- } accurate results with coarse mesh

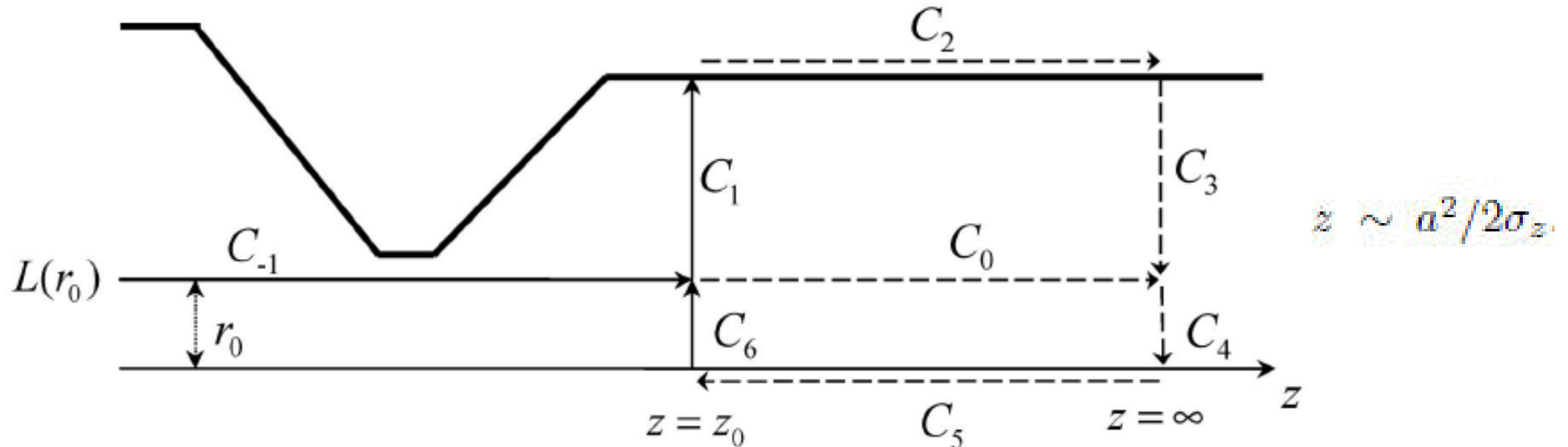


- in **3D** only solver, modelling and meshing in CST Microwave Studio
- allows for accurate calculations on conventional single-processor PC
- To be parallelized ...

Indirect Integration Algorithm

O. Napoly, Part. Accel. **36**, 15 (1991).

O. Napoly, Y. Chin, and B. Zotter, Nucl. Instrum. Methods Phys. Res., Sect. A **334**, 255 (1993).



$$\begin{aligned}
 QW_{\parallel}^{(m)} = & - \int_{C_{-1}} e_z^{(m)} dz + \frac{\beta}{2a^m} \int_0^a r^m [e_r + cb_{\theta} - e_{\theta} + cb_r]^{(m)} dr \\
 & - \frac{1}{2} \int_{r_0}^a \left\{ \left(\frac{r_0^m}{r^m} + \frac{r_0^{-m}}{r^{-m}} \right) [e_r + cb_{\theta}]^{(m)} + \left(\frac{r_0^m}{r^m} - \frac{r_0^{-m}}{r^{-m}} \right) [e_{\theta} - cb_r]^{(m)} \right\} dr
 \end{aligned}$$

PHYSICAL REVIEW SPECIAL TOPICS - ACCELERATORS AND BEAMS
9, 102002 (2006)

Indirect methods for wake potential integration

Igor Zagorodnov



Indirect Integration Algorithm

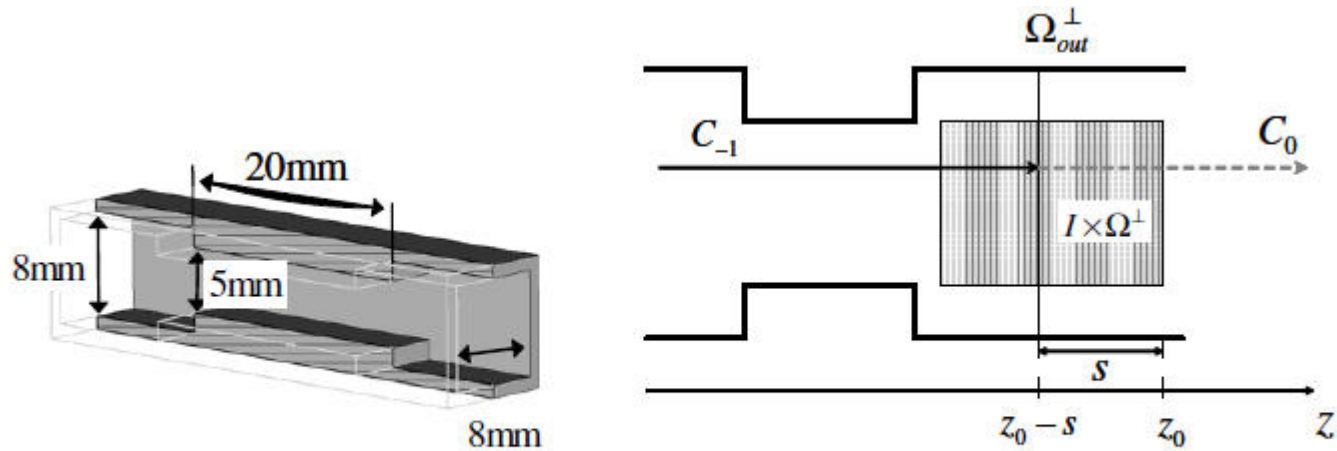
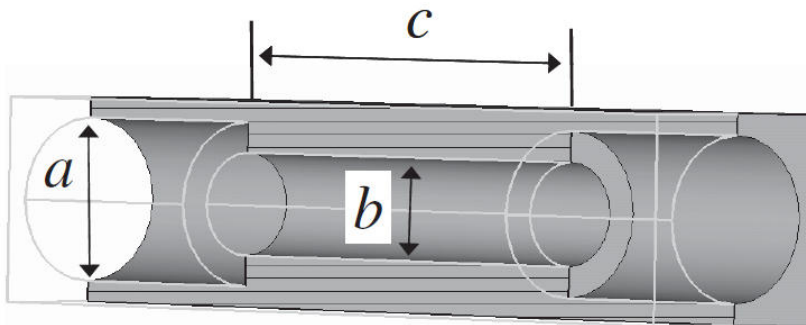


FIG. 5. The rectangular collimator. Contour C_{-1} for direct integration and cross section Ω_{out}^\perp for indirect integration algorithm.

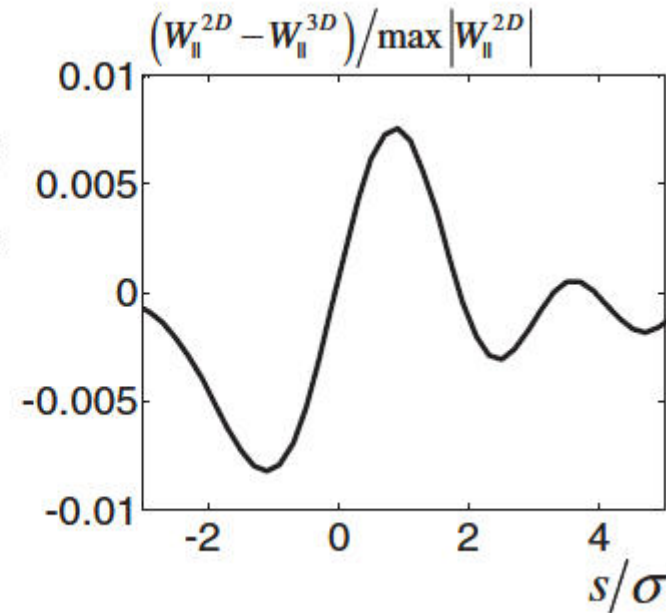
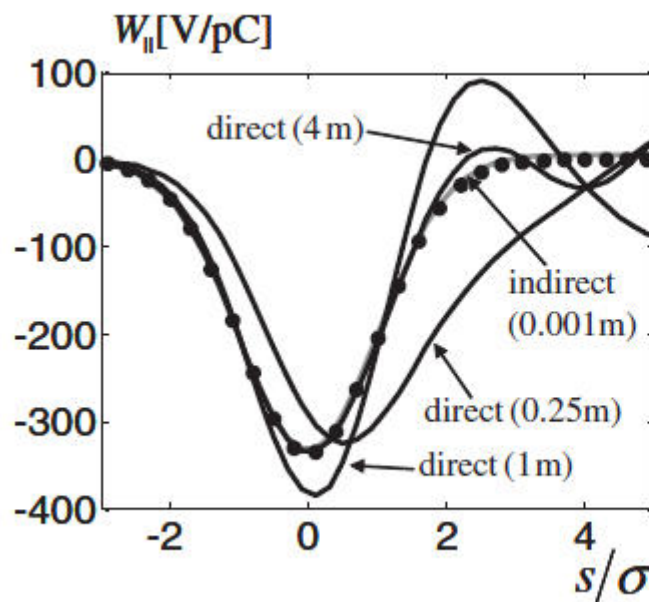
$$QW_{\parallel}(\vec{r}_0, s) = - \int_{C_{-1}(\vec{r}_0, z_0 - s)} E_z^{sc}[\vec{r}_0, z, t(z, s)] dz - u(\vec{r}_0, s), \quad t(z, s) = \frac{z + s}{c}$$

$$\Delta u(\vec{r}, s) = - \left[\frac{\partial}{\partial s} + \frac{\partial}{c \partial t} \right] E_z^{sc}(\vec{r}, z_0 - s, t_0), \quad \vec{r} \in \Omega_{out}^\perp, \quad u(\vec{r}, s) = 0, \quad \vec{r} \in \partial \Omega_{out}^\perp$$

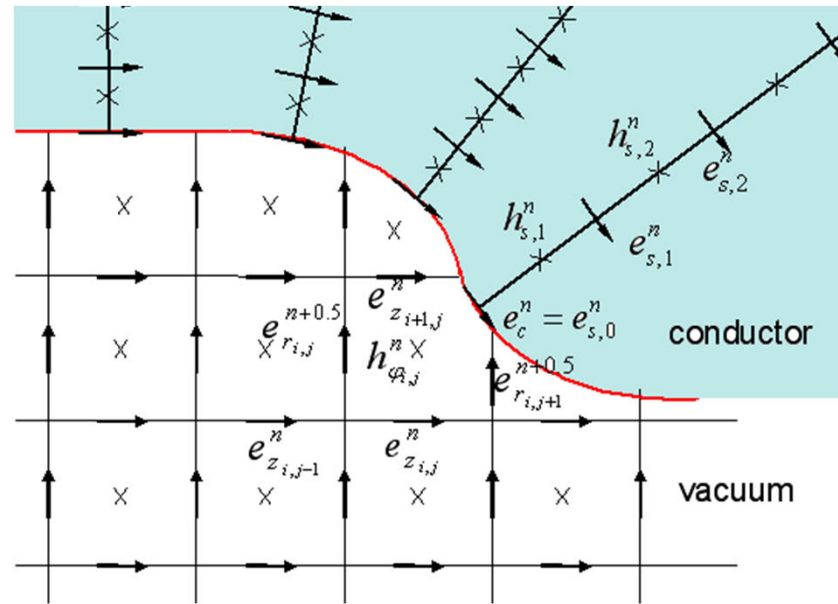
Indirect Integration Algorithm



$a = 8 \text{ mm}$, $b = 5 \text{ mm}$, and $c = 20 \text{ mm}$



Modelling of Conductive Walls



PHYSICAL REVIEW SPECIAL TOPICS - ACCELERATORS AND BEAMS 15, 054401 (2012)

Hybrid TE-TM scheme for time domain numerical calculations of wakefields in structures with walls of finite conductivity

Andranik Tsakanian

CANDLE, Acharyan 31, 0040, Yerevan, Armenia

Martin Dohlus and Igor Zagorodnov

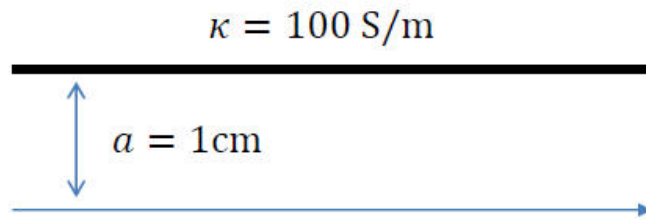
DESY, Notkestrasse 85, 22607, Hamburg, Germany

(Received 23 February 2011; published 9 May 2012)



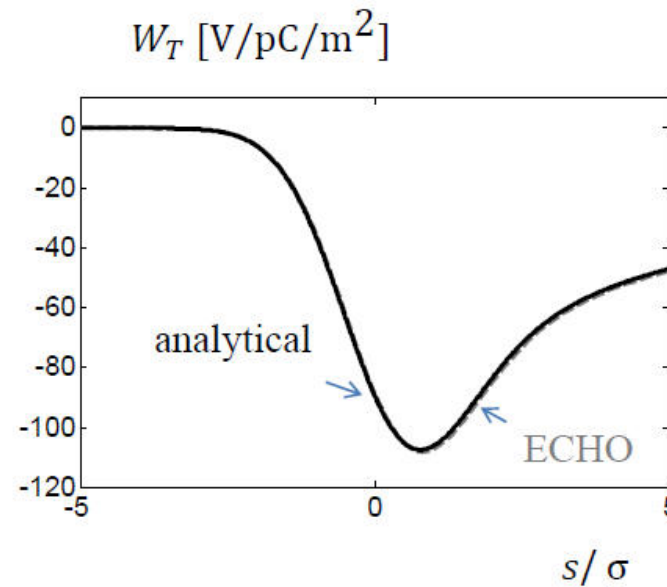
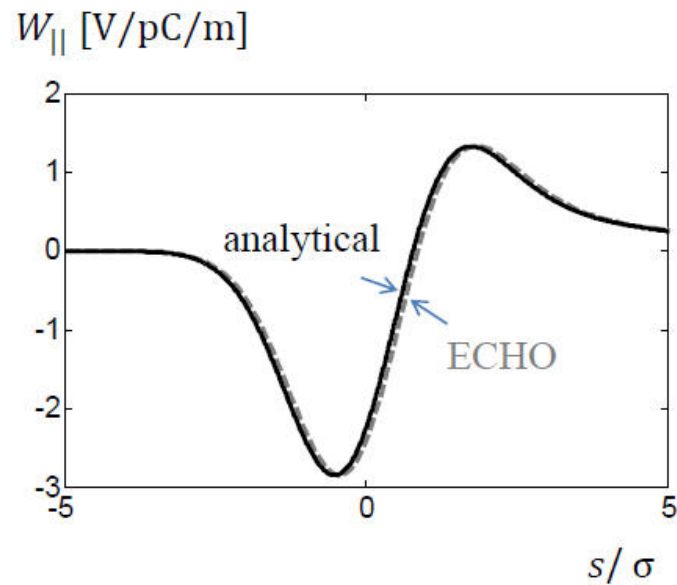
Modelling of Conductive Walls

Steady-state wake in the pipe

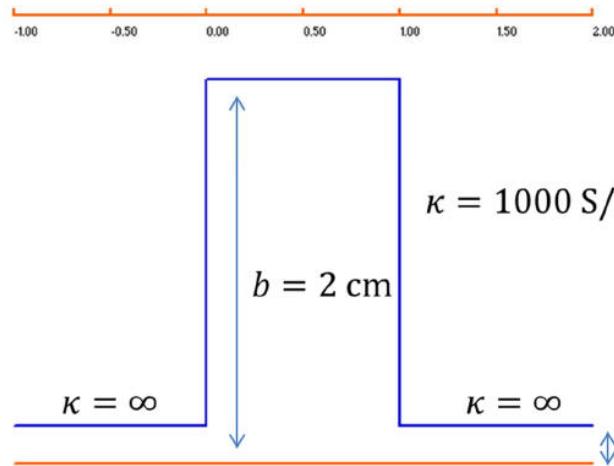


Gaussian bunch with RMS length
 $\sigma = 1 \text{ mm}$

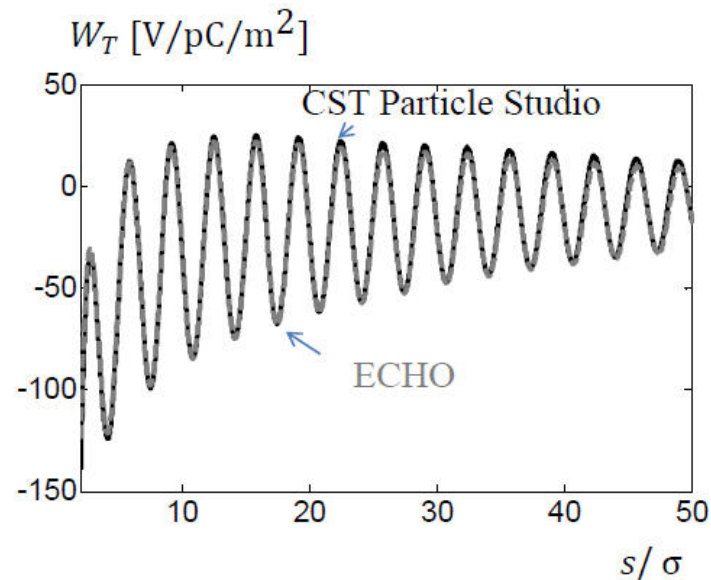
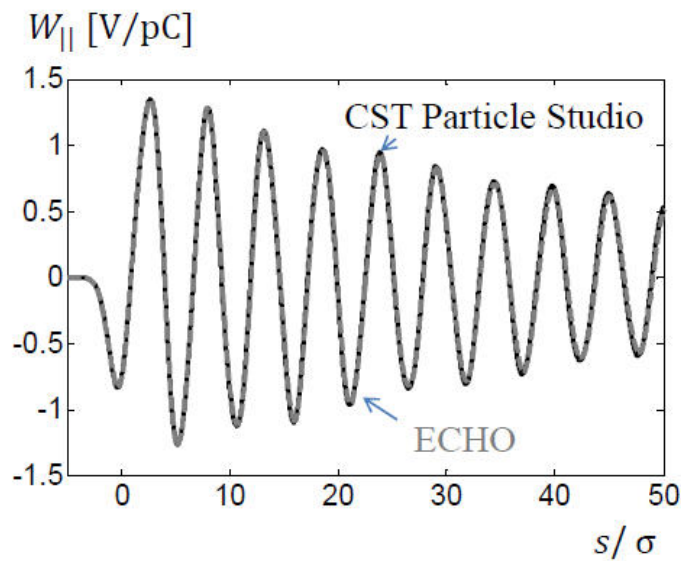
ECHO result is a difference between the wakes for a pipe of 2 m and a pipe of 1 m.



Modelling of Conductive Walls

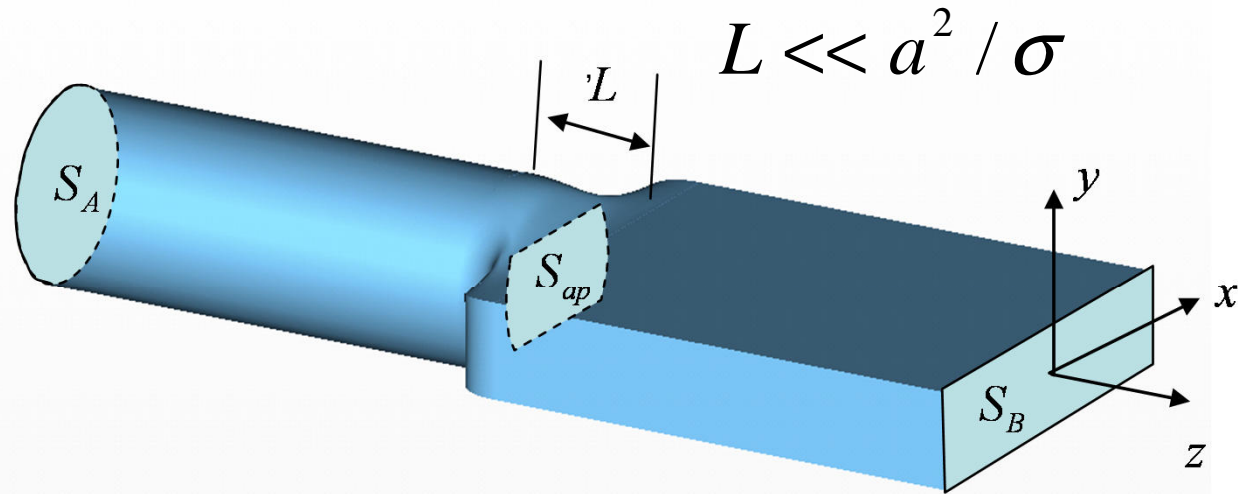


Gaussian bunch with RMS length
 $\sigma = 1 \text{ cm}$



Optical Approximation

G. Stupakov, K. Bane, and I. Zagorodnov, Phys. Rev. ST Accel. Beams 10, 054401 (2007).



$$Z_{\parallel}(\mathbf{r}_1, \mathbf{r}_2) = \frac{2\epsilon_0}{c} \left[\int_{S_B} \nabla \varphi_B(\mathbf{r}_1, \mathbf{r}) \nabla \varphi_B(\mathbf{r}_2, \mathbf{r}) ds - \int_{S_{ap}} \nabla \varphi_A(\mathbf{r}_1, \mathbf{r}) \nabla \varphi_B(\mathbf{r}_2, \mathbf{r}) ds \right]$$

$$\Delta \varphi_A(\mathbf{r}_i, \mathbf{r}) = -\epsilon_0^{-1} \delta(\mathbf{r} - \mathbf{r}_i)$$

$$\mathbf{r} \in S_A$$

$$\varphi_A(\mathbf{r}_i, \mathbf{r}) = 0$$

$$\mathbf{r} \in \partial S_A$$

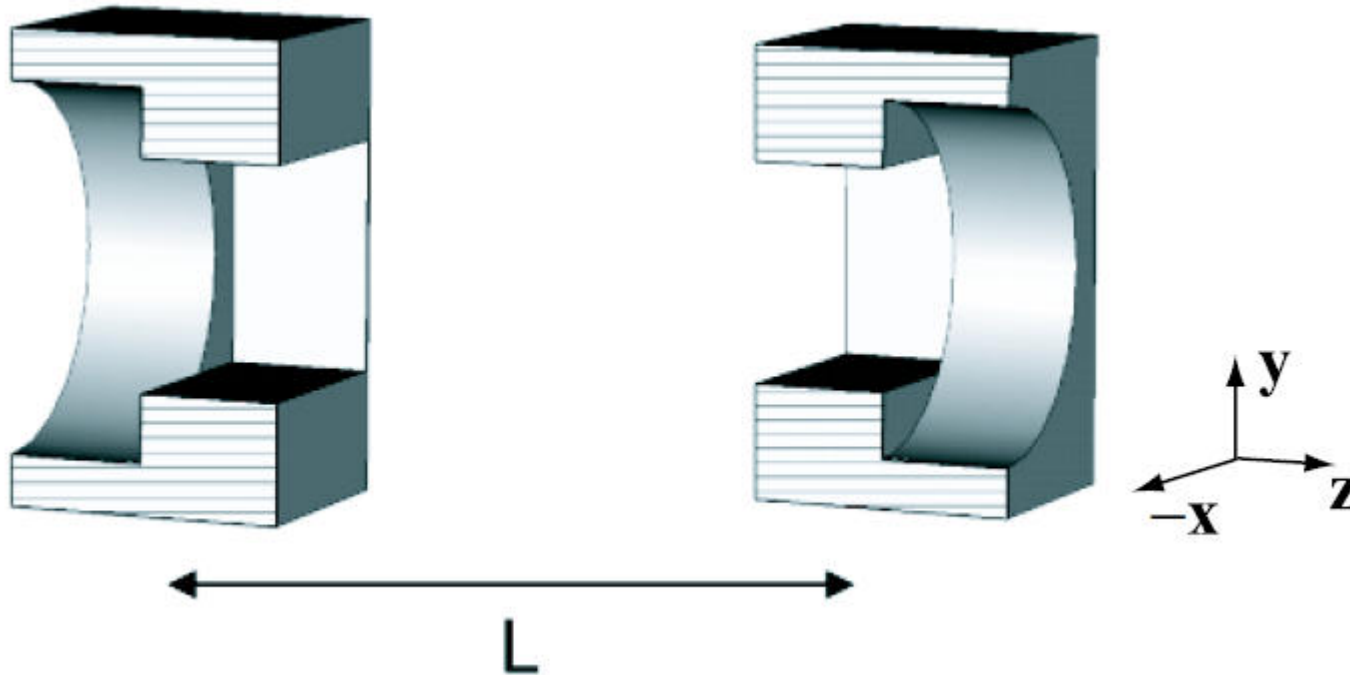
$$\Delta \varphi_B(\mathbf{r}_i, \mathbf{r}) = -\epsilon_0^{-1} \delta(\mathbf{r} - \mathbf{r}_i) \quad i = 1, 2$$

$$\mathbf{r} \in S_B$$

$$\varphi_B(\mathbf{r}_i, \mathbf{r}) = 0$$

$$\mathbf{r} \in \partial S_A$$

Optical Approximation



K. L. F. Bane and I. Zagorodnov, in Proceedings of the European Particle Accelerator Conference, Edinburgh, 2006, pp. 2952–2954.

Optical Approximation

PHYSICAL REVIEW SPECIAL TOPICS - ACCELERATORS AND BEAMS
10, 074401 (2007)

Impedance calculations of nonaxisymmetric transitions using the optical approximation

K. L. F. Bane and G. Stupakov

Stanford Linear Accelerator Center, Stanford University, Stanford, California 94309, USA

I. Zagorodnov

Deutsches Elektronen-Synchrotron, Notkestrasse 85, 22603 Hamburg, Germany
(Received 5 March 2007; published 10 July 2007)

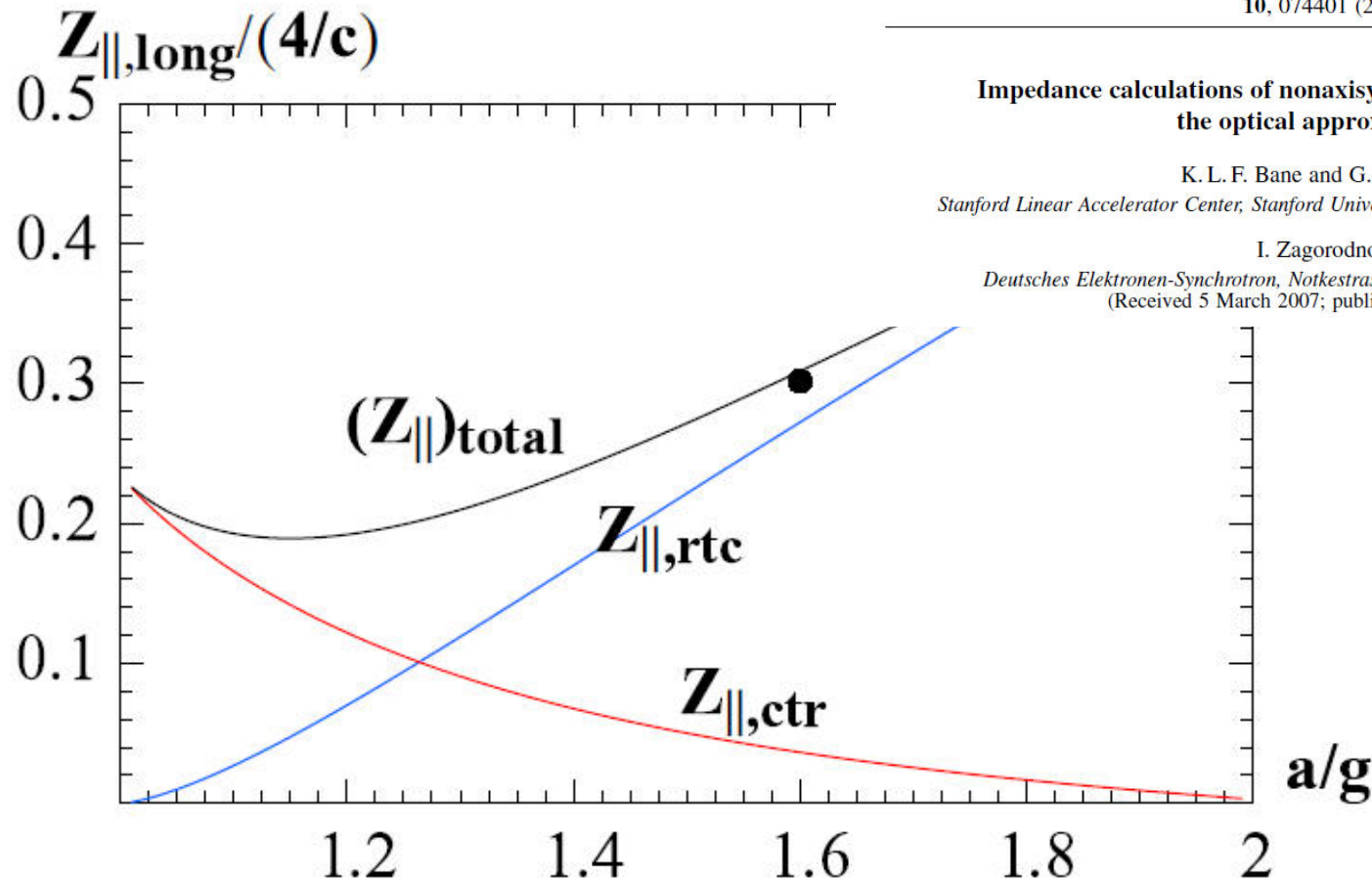
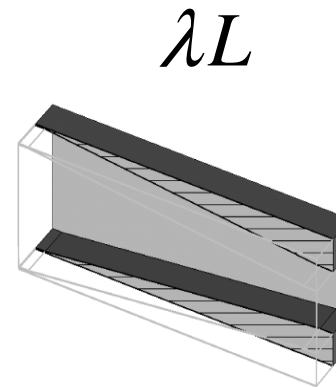
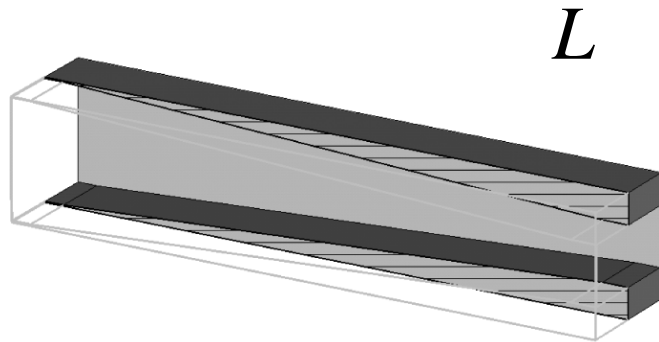


FIG. 20. (Color) Longitudinal impedance for transitions of the LCLS rectangular-to-circular type, giving $Z_{\parallel, \text{rtc}}$, $Z_{\parallel, \text{ctr}}$, and their sum $(Z_{\parallel})_{\text{total}}$ as functions of circular radius a . The rectangle width $2w = 4g$. The ECHO result for $(Z_{\parallel})_{\text{total}}$, from Ref. [9], is given by the black dot.



Slowly Tapered Transitions



$$W(s, \sigma_z) = \frac{1}{\lambda} W_\lambda\left(\frac{s}{\lambda}, \frac{\sigma_z}{\lambda}\right)$$

$$W_\perp(s, \sigma_z) = W_{\perp\lambda}\left(\frac{s}{\lambda}, \frac{\sigma_z}{\lambda}\right)$$

PHYSICAL REVIEW SPECIAL TOPICS - ACCELERATORS AND BEAMS
14, 014402 (2011)

Impedance scaling for small angle transitions

G. Stupakov and K.L.F. Bane

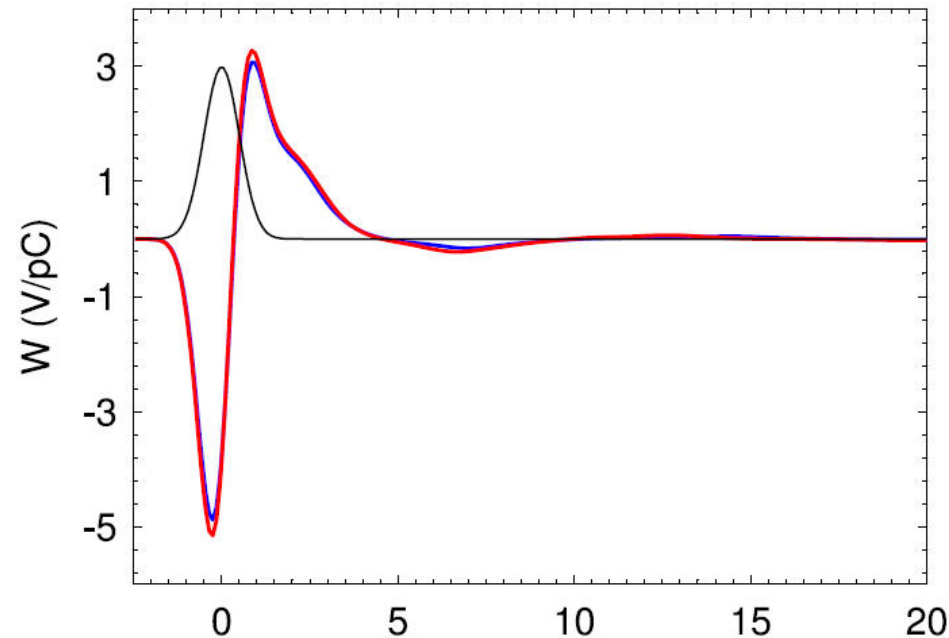
SLAC National Accelerator Laboratory, Stanford University, Stanford, California 94309, USA

I. Zagorodnov

Deutsches Elektronen-Synchrotron, Notkestrasse 85, 22603 Hamburg, Germany
(Received 24 September 2010; published 10 January 2011)

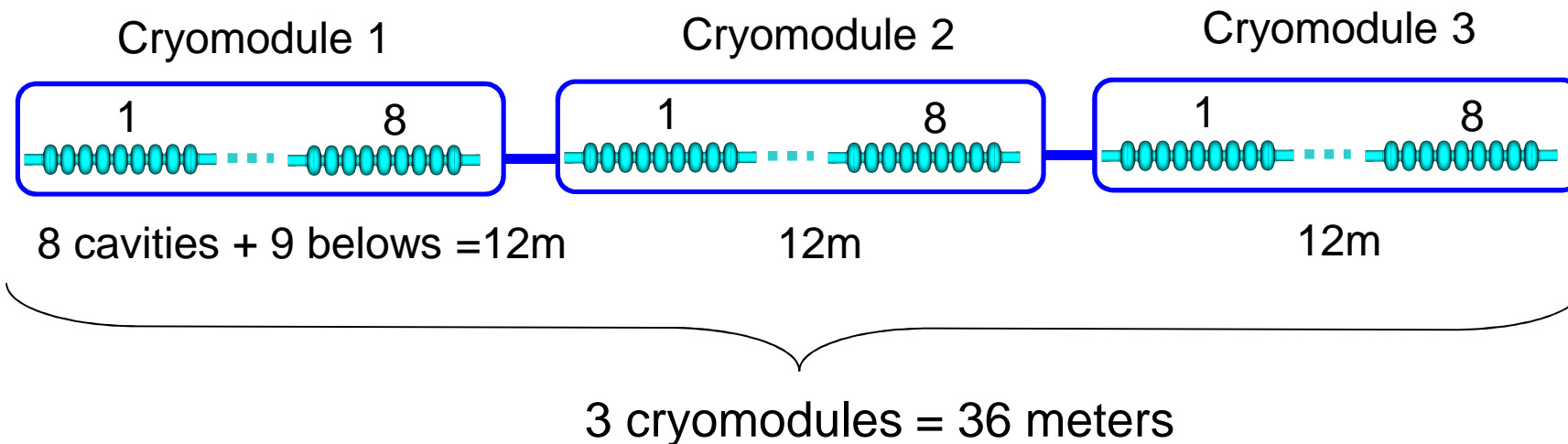


Slowly Tapered Transitions



As a 3D (noncylindrically symmetric) example we consider a longitudinally symmetric, small angle transition, from a large beam pipe to a small one and then back again, with the central region taken to be infinitely long. In the horizontal (x) direction the beam pipe remains unchanged; the transition occurs only in the vertical (y) direction. For the nominal geometry, the large beam pipe has a square cross section of 30 mm by 30 mm ($x \times y$), the small one is rectangular with dimensions 30 mm by 15 mm, and the central region is assumed to be long. The connecting pipes are straight line tapers (in y) of angle 3° (see Fig. 7). The nominal bunch length $\sigma_z = 0.5$ mm. For the scaled case we take $\lambda = \frac{1}{2}$.

Cavity and Coupler Wakes



Transverse wakes for short bunches up to $\sigma = 50\mu m$ have been studied.

To reach steady state solution the structure from 3 cryomodules is considered.

For longitudinal case the wakes were studied earlier by Novokhatski et al*. The transverse results are calculated with ECHO**.

*Novokhatski A, Timm M, Weiland T. *Single Bunch Energy Spread in the TESLA Cryomodule*, DESY, TESLA-1999-16, 1999

**Weiland T., Zagorodnov I, *The Short-Range Transverse Wake Function for TESLA Accelerating Structure*, DESY, TESLA-2003-19, 2003

Cavity and Coupler Wakes

The wake functions at short distance are approximately related by

$$w_{\perp}^1(s) \cong \frac{2}{a^2} \int_0^s w_{\parallel}^0(z) dz \quad (1)$$

$$\partial_s w_{\perp}^1(0) \cong \frac{2}{a^2} w_{\parallel}^0(0) \quad (2)$$

K.L.F.Bane,
SLAC-PUB-
9663, LCC-0116,
2003

Different behavior!

One-cell structure

$$w_{\parallel}(s) = \frac{Z_0 c}{\sqrt{2} \pi^2 a} \sqrt{\frac{g}{s}} \sim O(s^{-0.5})$$

$$w_{\perp}(s) = \frac{2}{a^2} \frac{\sqrt{2} Z_0 c}{\pi^2 a} \sqrt{g s} \sim O(s^{0.5})$$

Periodic structure

$$w_{\parallel}(s) = A \frac{Z_0 c}{\pi^2 a} \exp(-\sqrt{s/s_0}) \sim O(1)$$

$$w_{\perp}(s) = \frac{2}{a^2} A \frac{Z_0 c}{\pi^2 a} 2s_1 \left(1 - \left(1 + \sqrt{s/s_1} \right) e^{-\sqrt{s/s_1}} \right) \sim O(s)$$

A, s_0, s_1 - fit parameters

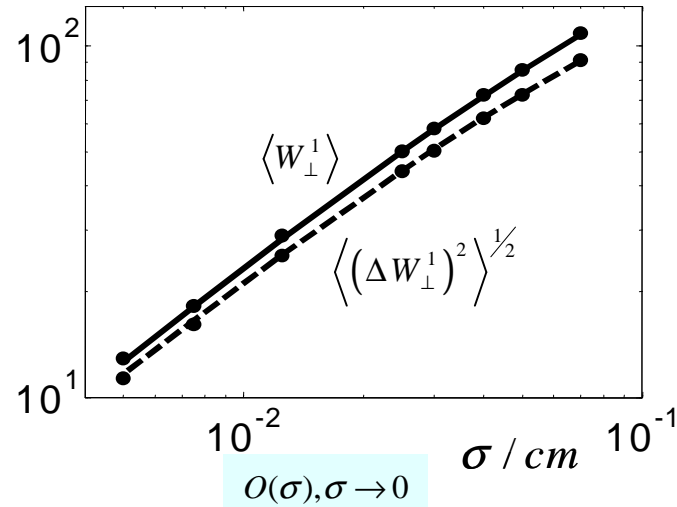
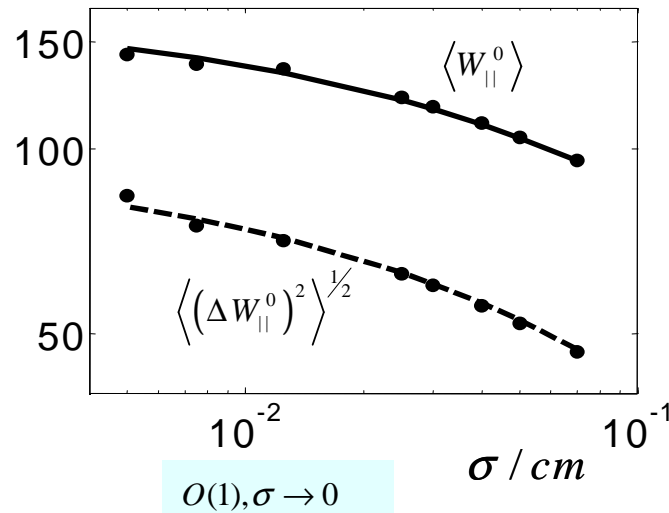
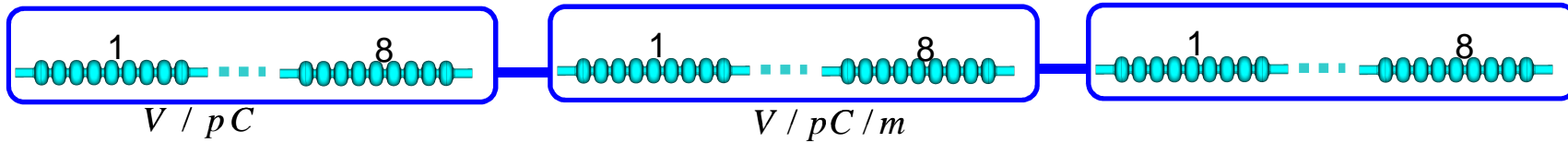
a – iris radius, g – cavity gap

$s_0 = s_1$ – relations (1), (2) hold exactly

$s_0 \neq s_1$ – only relation (2) holds exactly



Cavity and Coupler Wakes



Comparison of numerical (points) and analytical (lines) integral parameters for the third cryomodule

Like periodic structure!

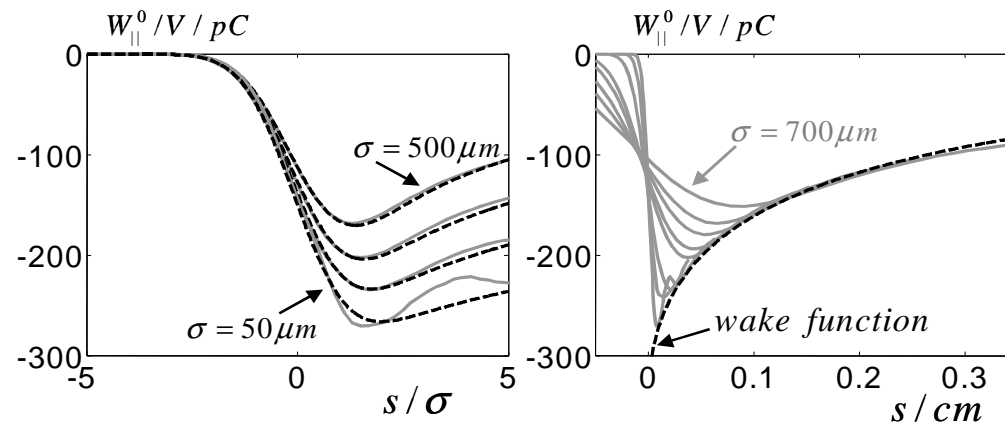
$$w_{||}(s) = 344 \exp(-\sqrt{s/s_0}) [\text{V/pC/module}] \quad O(1), s \rightarrow 0$$

$$w_{\perp}(s) = 10^3 \left(1 - \left(1 + \sqrt{\frac{s}{s_1}} \right) \exp\left(-\sqrt{\frac{s}{s_1}}\right) \right) \left[\frac{\text{V}}{\text{pC} \times \text{m} \times \text{module}} \right] \quad O(s), s \rightarrow 0$$

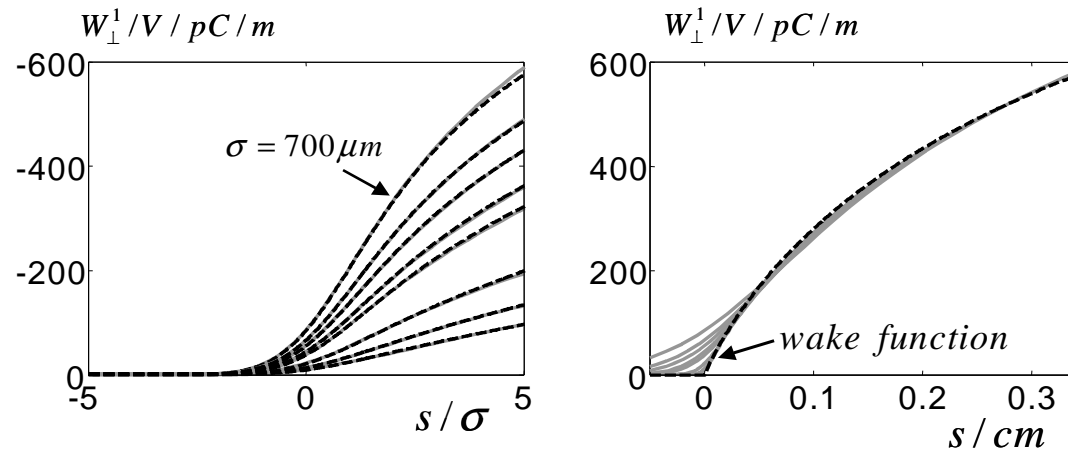
$$s_0 = 1.74 \cdot 10^{-3} \quad s_1 = 0.92 \cdot 10^{-3} \quad A = 1.46 \quad a = \bar{a} = 35.57 \text{mm}$$



Cavity and Coupler Wakes



Comparison of numerical (grays) and analytical (dashes) longitudinal wakes for the third cryomodule



Comparison of numerical (grays) and analytical (dashes) transverse wakes



Cavity and Coupler Wakes

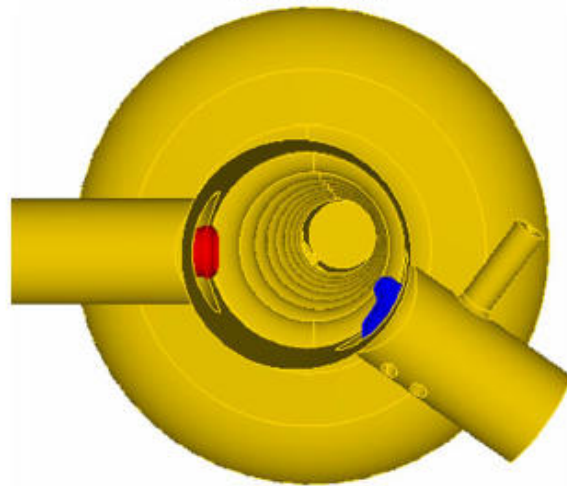
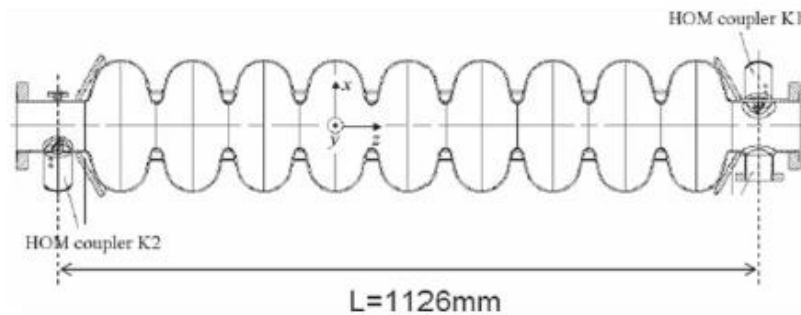


Figure 1: Sketch of an ILC cavity with the HM couplers (top). View from the downstream end of a cavity showing the FM coupler (red) and one HM coupler (blue).

WAKEFIELD AND RF KICKS DUE TO COUPLER ASYMMETRY IN TESLA-TYPE ACCELERATING CAVITIES *

K.L.F. Bane, C. Adolphsen, Z. Li, SLAC, Stanford, CA 94309, USA
 M. Dohlus, I. Zagorodnov, DESY, Hamburg, Germany
 I. Gonin, A. Lumin, N. Solyak, V. Yakovlev, FNAL, Batavia, IL 60510, USA
 E. Gjonaj, T. Weiland, TEMF, TU-Darmstadt, Germany

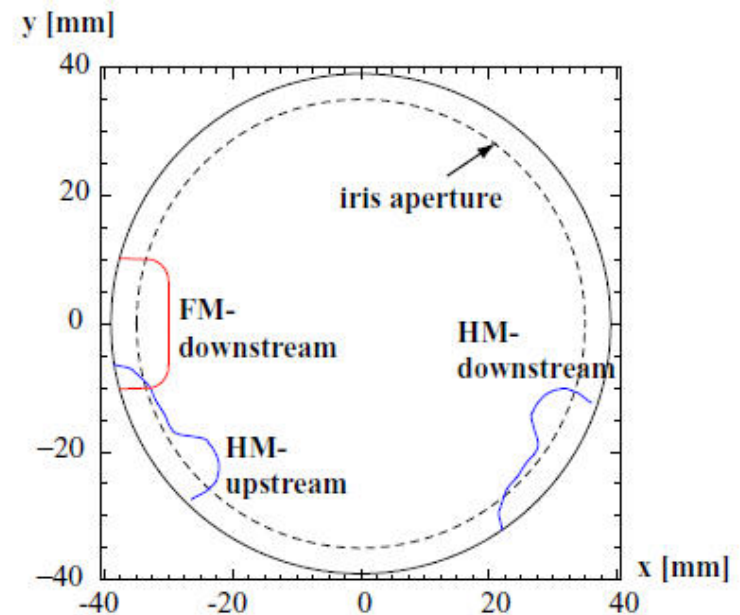


Figure 2: The profiles of the three couplers of a cavity, as seen from the downstream end. The solid circle is the coupler beam pipe, the dashed circle the iris aperture.

Cavity and Coupler Wakes

Table 1: Wake kick on-axis (k_{x0}, k_{y0}) due to coupler asymmetry, for bunch length $\sigma_z = 1$ mm, in [V/nC] (ECHO).

Case	Numerical	Analytical
Couplers in pipe	(-21.2, -18.6)	(-20.8, -17.1)
Couplers in cavity	(-10.8, -10.0)	(-12.7, -7.0)
Steady-state solution	(-7.6, -6.8)	

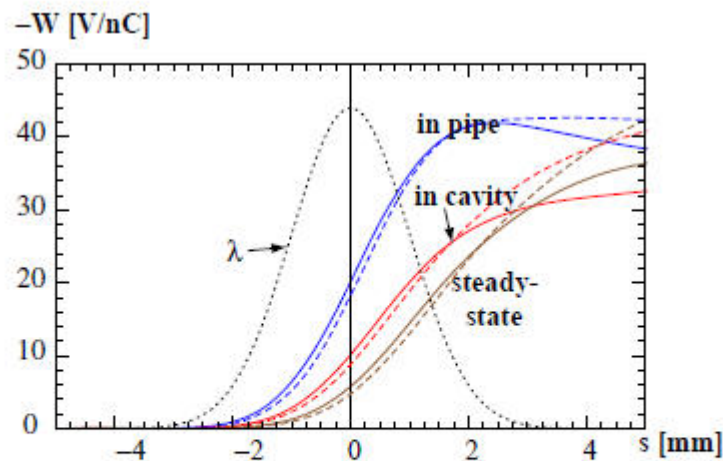


Figure 3: Plots of $-W_{x0}(s)$ (solid) and $-W_{y0}(s)$ (dashed) for couplers in pipe, in cavity, and the steady-state solution, for $\sigma_z = 1$ mm (ECHO). Dots indicate bunch shape.

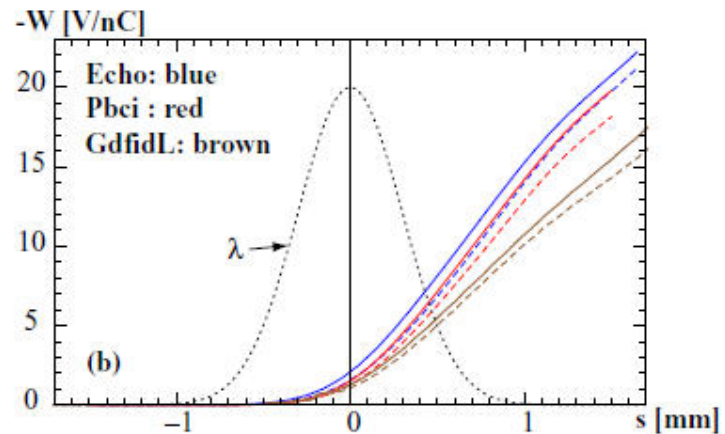
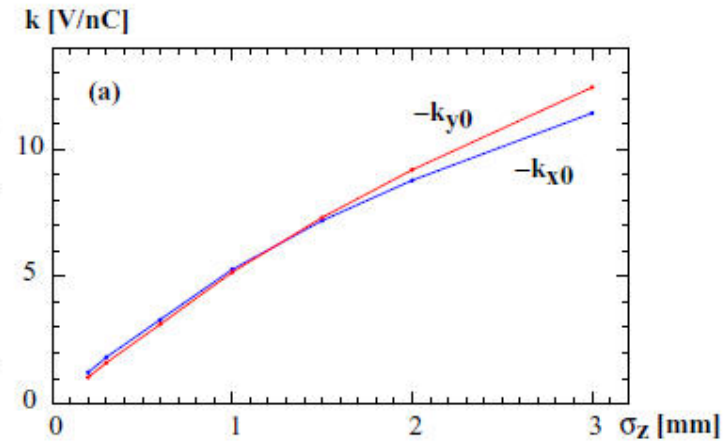
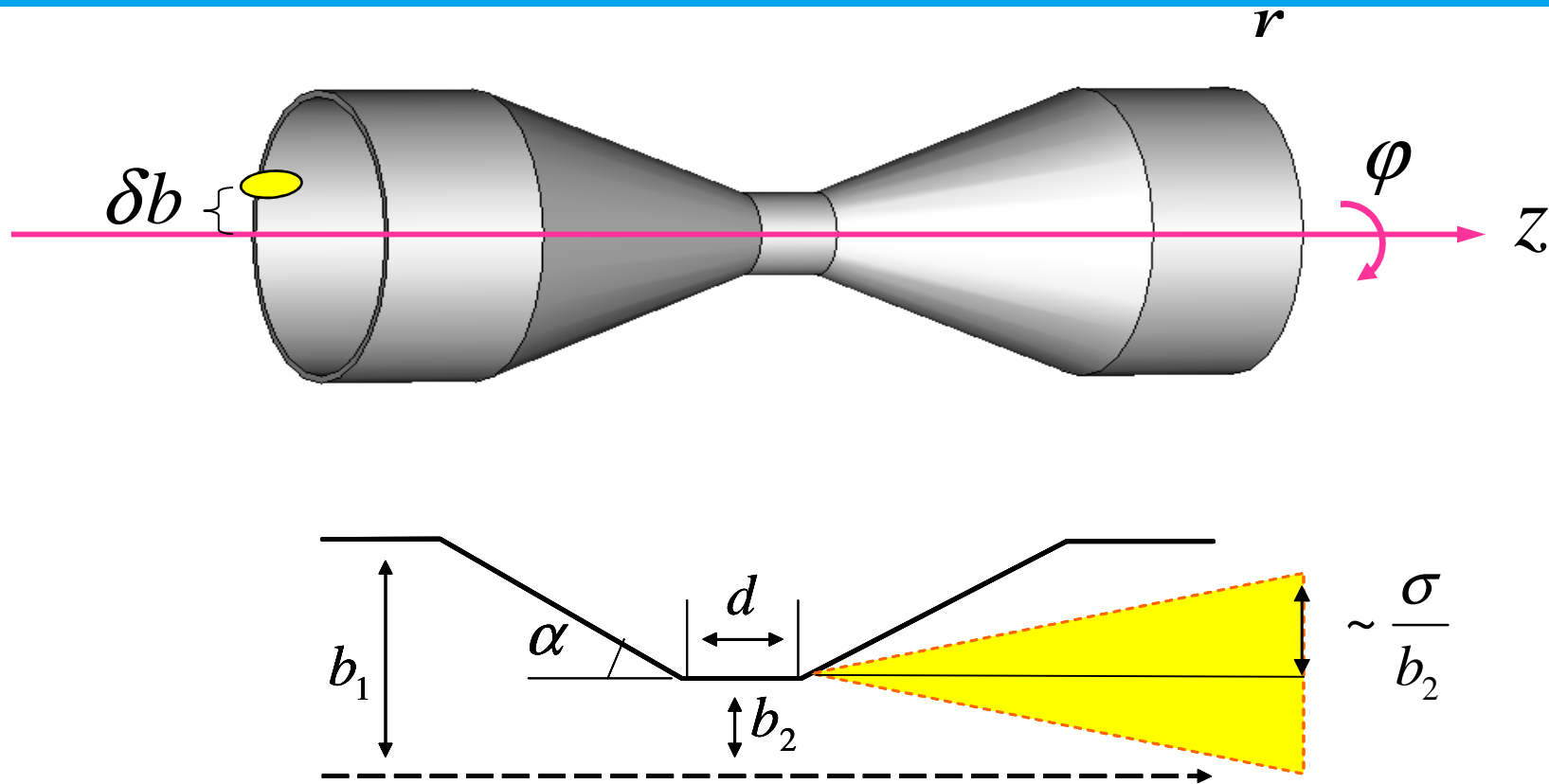


Figure 4: The steady-state solution: (a) on-axis kick factor as function of σ_z (GdfidL); (b) $-W_{x0}(s)$ (solid), $-W_{y0}(s)$ (dashed) for $\sigma_z = 300$ μm . Dots indicate bunch shape.

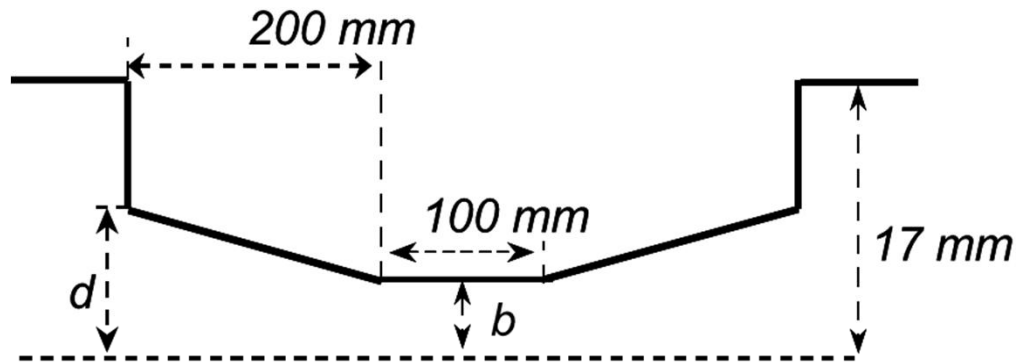
Collimator Wakes



K. Yokoya, *Impedance of Slowly Tapered Structures*, Tech. Rep. SL/90-88 (AP), CERN, 1990.

Collimator Wakes

The geometry optimization with regard to the near-axis wakefields ($\sigma=50\mu\text{m}$)

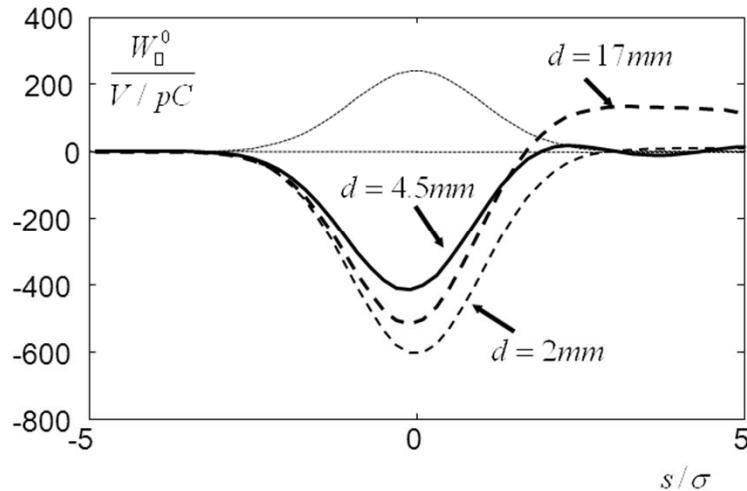


Optimal parameters

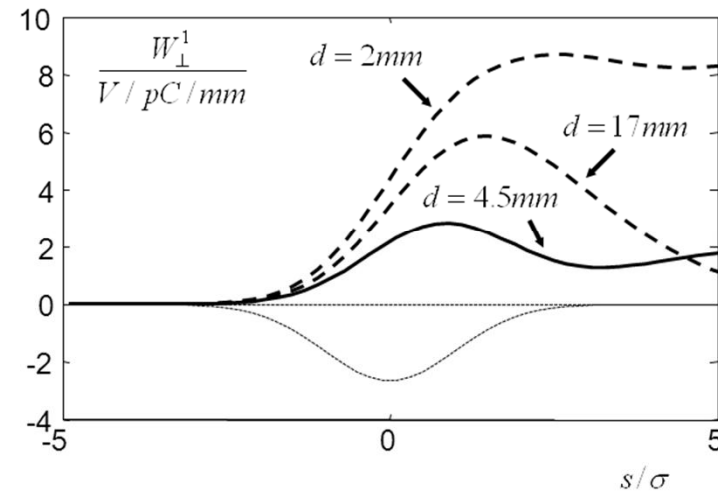
b, mm	2	3	6
d, mm	4.5	5.5	10

Geometry of the "step+taper" collimator

I. Zagorodnov et al, DESY, TESLA-2003-19, 2003



The longitudinal wakes for the aperture $b=2$ mm

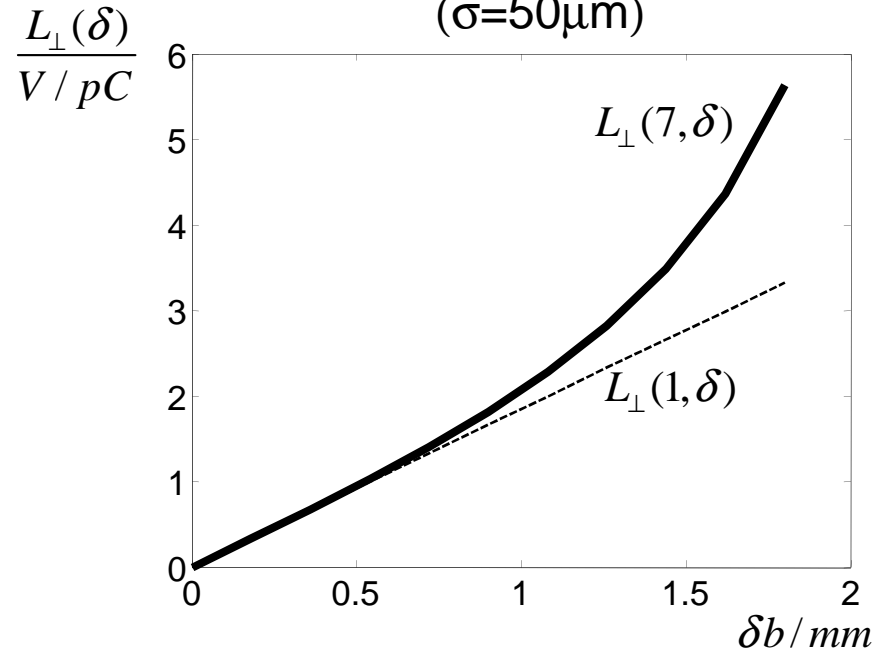


The transverse wakes for the aperture $b=2$ mm

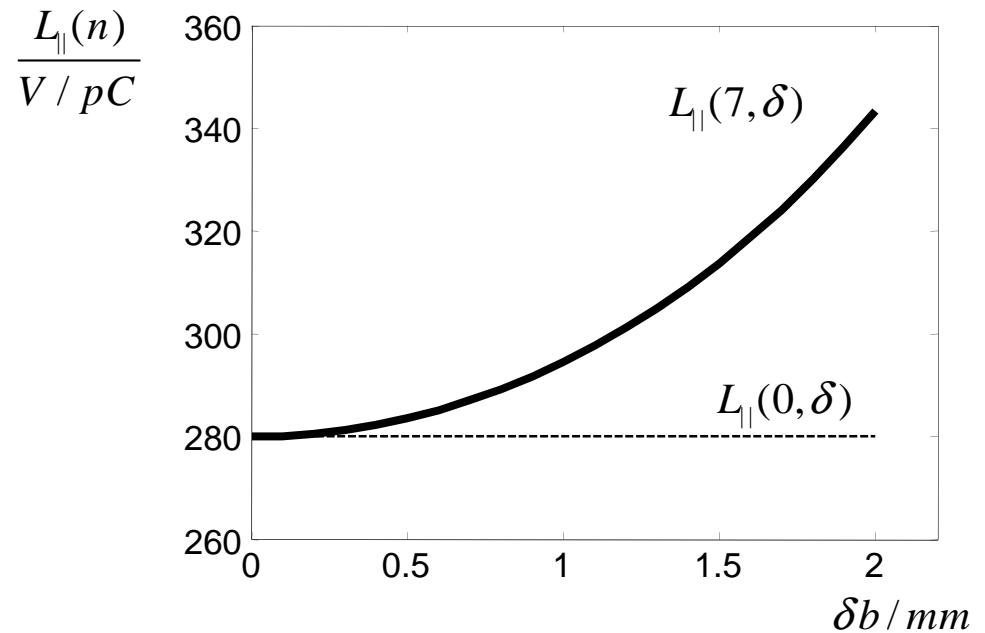


Collimator Wakes

Near-wall wakefields of the optimized geometry
($\sigma=50\mu\text{m}$)



The kick factor for the aperture $b=2$ mm



The loss factor for the aperture $b=2$ mm

The loss factor increases only by ~20% up to the aperture wall.

The kick factor shows fast grows near the wall

$$-\ln(1-\delta^2), \quad \delta \rightarrow 1.$$



Collimator Wakes

Theory Review

Axially symmetric taper

$$Z_{\perp}(k) \cong -\frac{iZ_0}{2\pi} \int_{-\infty}^{\infty} dz \frac{r'(z)^2}{r(z)^2}$$

K. Yokoya, 1990

Flat rectangular taper $2w \times 2h, w \gg h$

$$Z_y^{rect}(k) = -\frac{iZ_0 w}{4} \int_{-\infty}^{\infty} dz \frac{h'(z)^2}{h(z)^3}$$

G. Stupakov, 1995

Elliptical x-section taper $2w \times 2h, w \gg h$

$$Z_x^{ell}(k) = -\frac{iZ_0}{4\pi} \int_{-\infty}^{\infty} dz \frac{h'(z)^2}{h(z)^2}$$

$$Z_y^{ell}(k) = -\frac{iZ_0 \pi w}{16} \int_{-\infty}^{\infty} dz \frac{h'(z)^2}{h(z)^3}$$

Z_x : $h \ll L, k \sim 1/h_{\min}$

Z_y : $w \ll L, k \sim 2/w_{\min}$

B. Podobedov & S. Krinsky, 2006

These are inductive regime impedances. Tapers are gradual to be effective.

Functionals lend themselves to simple boundary optimization.



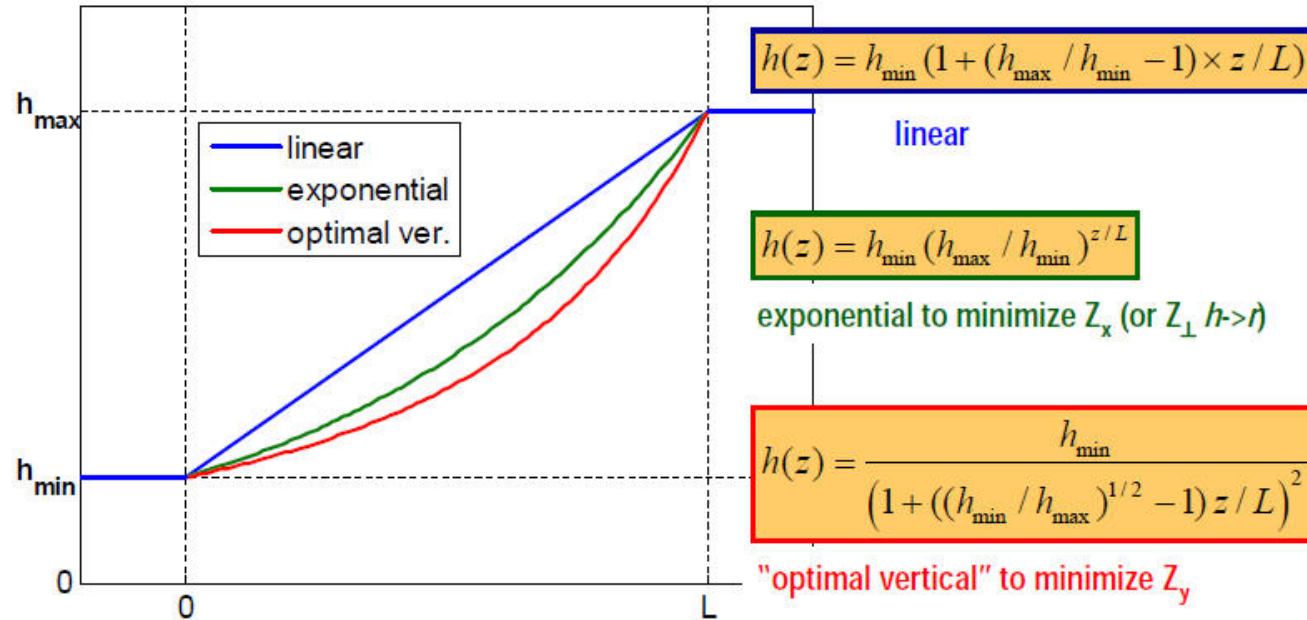
Collimator Wakes

IMPEDANCE MINIMIZATION BY NONLINEAR TAPERING

Boris Podobedov[#], BNL/NSLS, Upton, New York, USA

Igor Zagorodnov[&], DESY, Hamburg, Germany

Optimizing boundaries

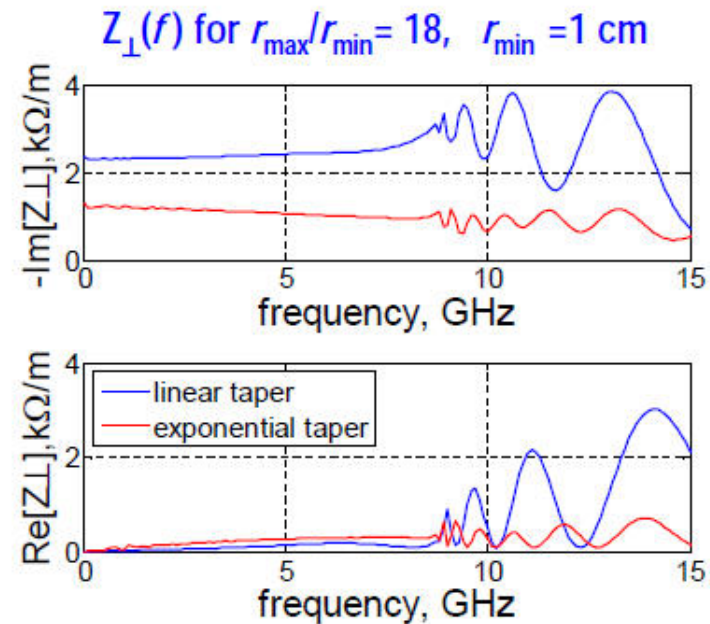
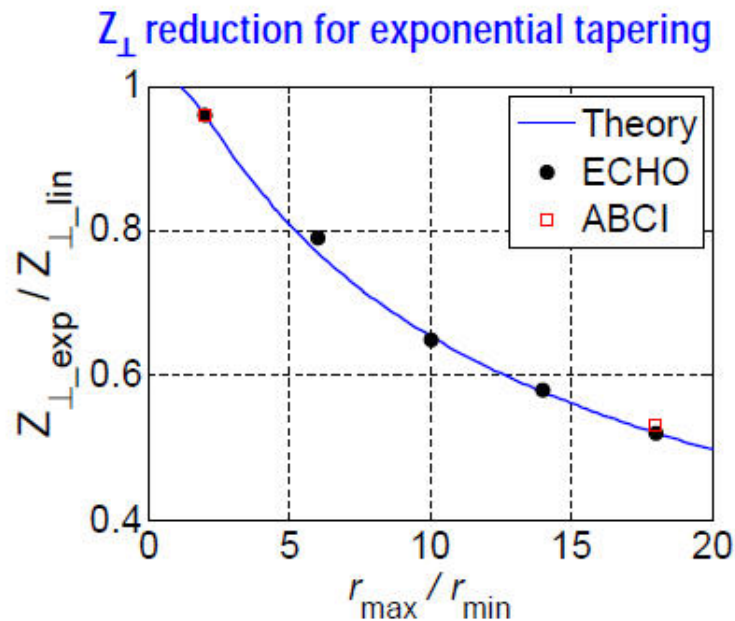


Reduced slope @ small $h(z)$; big difference when $h_{\max}/h_{\min} \gg 1$
 At $h_{\max}/h_{\min} = 20$ predict factor of 2 reduction for Z_{\perp} or Z_x , factor of ~3 for Z_y



Collimator Wakes

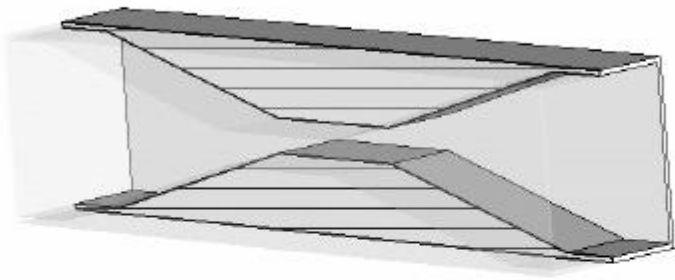
Impedance Reduction for Axially Symmetric Tapers



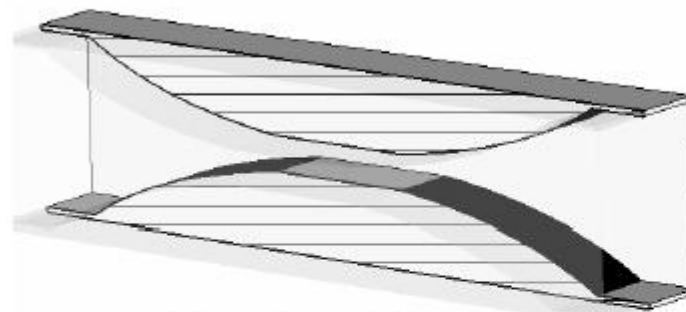
$Z_{\perp}[\text{k}\Omega/\text{m}]$ and reduction due to exponential taper agree well with theory
Impedance reduction extends through inductive regime ($k \sim 1/r_{\text{min}}$) & beyond

Collimator Wakes

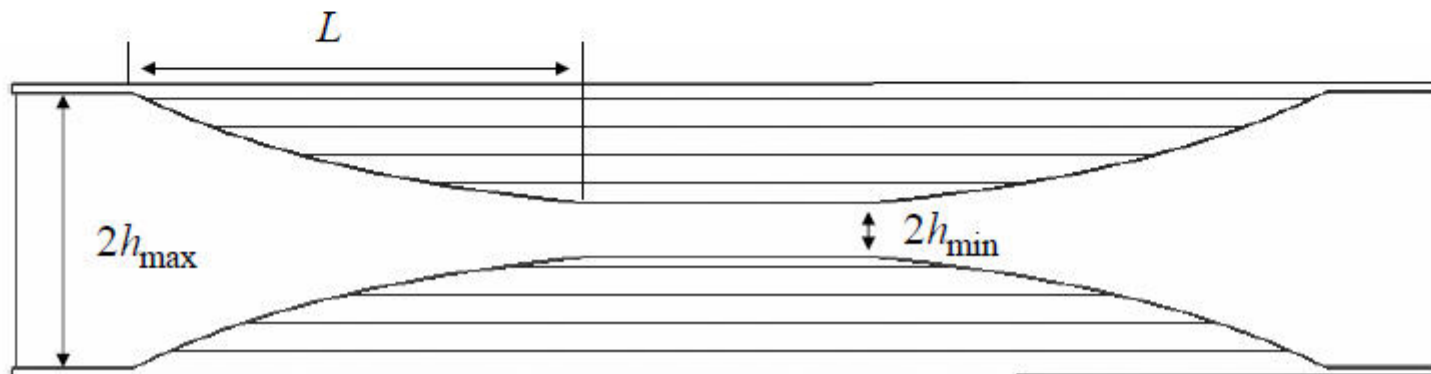
Geometry for Rectangular Taper Calculations



Linear taper

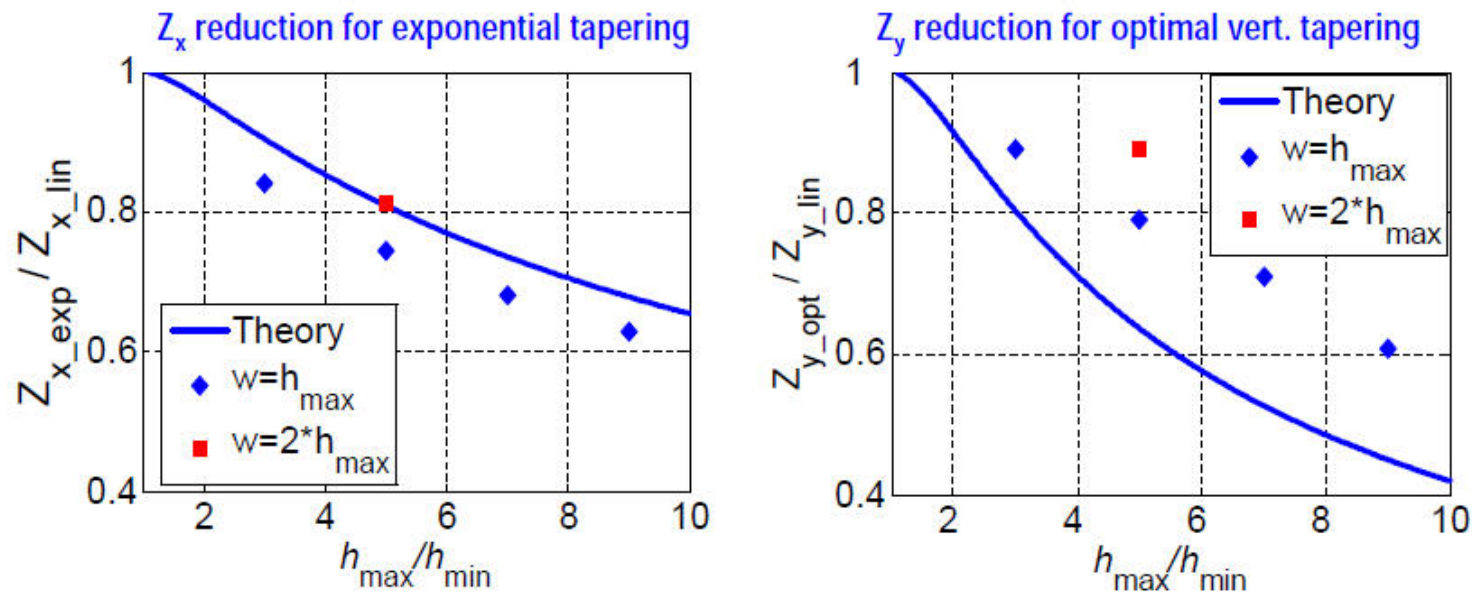


"Optimal" taper



Collimator Wakes

Impedance Reduction for Rectangular X-Section Tapers



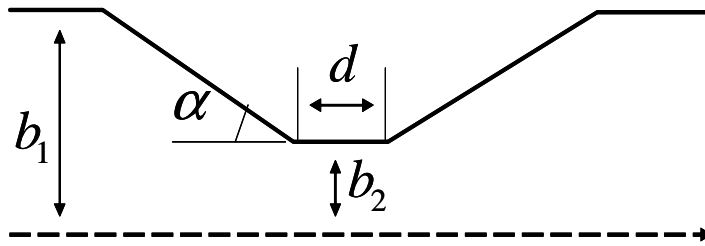
Z_x [k Ω /m] and reduction due to exponential taper agree well with theory

Z_y [k Ω /m] is less than theory; Z_y gets reduced due to optimal taper less than predicted

Results are very similar to elliptical structure




Collimator Wakes



- Regimes
- diffractive
 - inductive
 - intermediate

Figure 1: Top half of a symmetric collimator.

round		rectangular
$\rho_1 \equiv \alpha b_2 \sigma^{-1} \ll 1$	Inductive	$\rho_1 \ll 1, \rho_2 \equiv \alpha h^2 \sigma^{-1} b_2^{-1} \ll 1$
$k_{\perp} = \frac{2\alpha}{\sqrt{\pi}\sigma} \left(\frac{1}{b_2} - \frac{1}{b_1} \right) \frac{Z_0 c}{4\pi}$ (1)		$k_{\perp} = \frac{\sqrt{\pi} \alpha h}{\sigma} \left(\frac{1}{b_2^2} - \frac{1}{b_1^2} \right) \frac{Z_0 c}{4\pi}$ (2)
Intermediate $\rho_1 \sim 1, \rho_2 \geq \pi^2$		
$k_{\perp} = 2.7A \sigma^{-0.5} b_2^{-1.5} \sqrt{\alpha} Z_0 c (4\pi)^{-1}$ (3)		
$\rho_1 \gg 1$	Diffractive	$\rho_1 \gg 1$
		

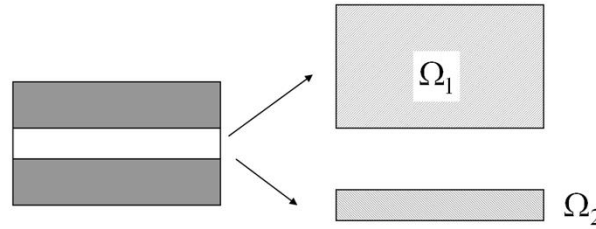
Collimator Wakes

Diffractive Regime

$$k_{\perp}^{short} \approx 0.5 k_{\perp}^{long}$$

$$Z_{\parallel} = 2Z^e \quad (4)$$

$$\begin{aligned} \Delta \varphi_i(\vec{x}) &= Z_0 Q \delta(\vec{x} - \vec{x}_0) & \vec{x}_i &\in \Omega_i \\ \varphi_i(\vec{x}) &= 0 & \vec{x}_i &\in \partial\Omega_i \quad i = 1, 2 \end{aligned}$$



long

$$Z^e = \frac{1}{Q^2 Z_0} \left(\int_{\Omega_1} \nabla \varphi_1^2 ds - \int_{\Omega_2} \nabla \varphi_2^2 ds \right) \quad (5)$$

short

$$Z^e = \frac{1}{Q^2 Z_0} \left(\int_{\Omega_1 - \Omega_2} \nabla \varphi_1^2 ds \right) \quad (6)$$

$$\begin{aligned} k_{\parallel} &= \frac{c}{\sqrt{\pi} \sigma} Z^e(0) \quad (7) \\ k_{\perp} &= c \Delta^{-2} (Z^e(\Delta) - Z^e(0)) \quad (8) \end{aligned}$$

long

$$k_{\perp} = \frac{Z_0 c}{2\pi} \left(\frac{1}{b_2^2} - \frac{1}{b_1^2} \right) \quad (11)$$

short

$$k_{\perp} = \frac{Z_0 c}{4\pi} \left(\frac{1}{b_2^2} - \frac{b_2^2}{b_1^4} \right) \quad (12)$$

$$k_{\parallel} = 0.5 \pi^{-1.5} \sigma^{-1} c Z_0 \log(b_1 b_2^{-1}) \quad (10)$$

Collimator Wakes

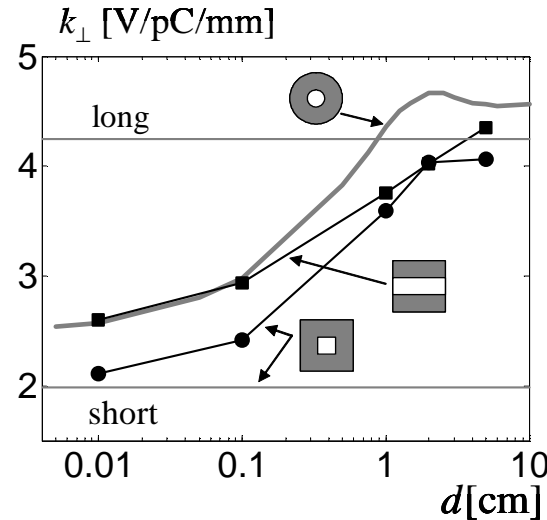
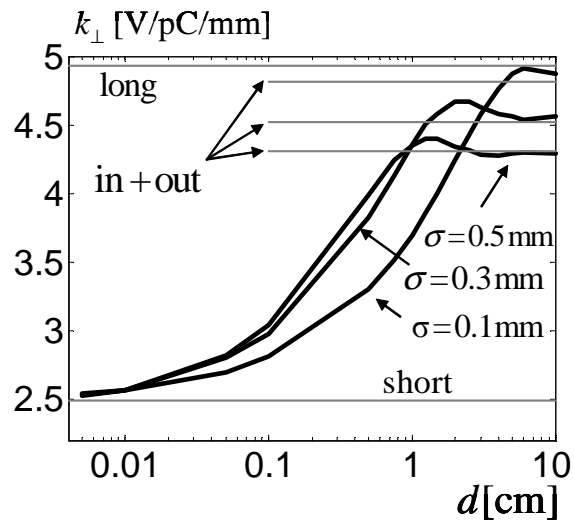


Table1: Loss and kick factors as estimated by 2D electrostatic calculation. The bunch length $\sigma = 0.3$ mm. ``Short'' means using Eq. 6, ``long'' Eq. 5

Type	$k_{//}$ [V/pC]		k_{tr} [V/pC/mm]	
	short	long	short	long
round	78	78	2.50	5.01
rect.	56	72	2.43	6.11
square	74	78	1.99	4.25

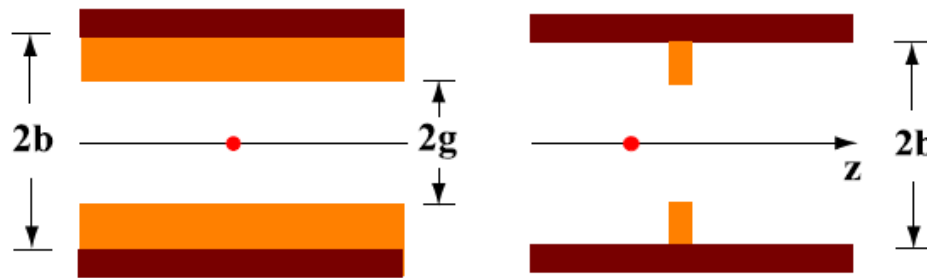
Figure 2: Kick factor vs. collimator length. A round collimator (left), a square or rectangular collimator ($\sigma = 0.3$ mm, right).

The good agreement we have found between direct time-domain calculation [1] and the approximations (5, 6), suggests that the latter method can be used to approximate short-bunch wakes for a large class of 3D collimators.



Collimator Wakes

I4: flat iris in flat beam pipe; longitudinal view

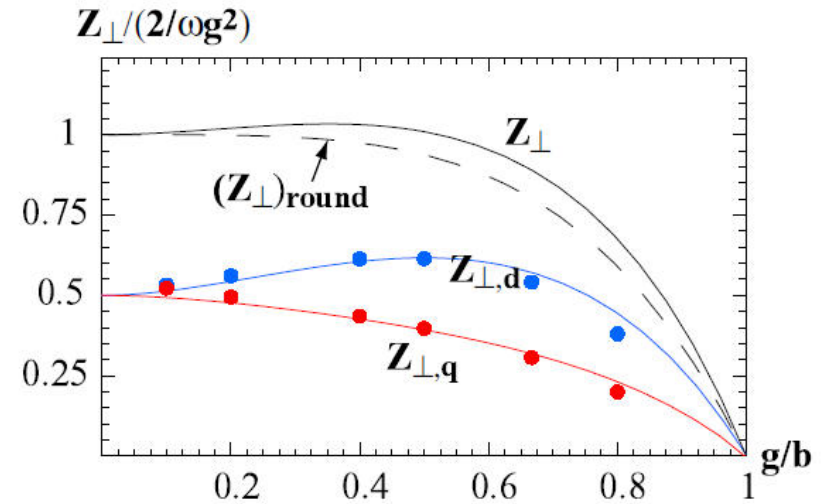


$$Z_{\perp, \text{tot}} = Z_{\perp, m} + y_1 Z_{\perp, d} + y_2 Z_{\perp, q}$$

The final solution is

$$\begin{aligned} Z_{\perp, d} &= \frac{\pi \alpha^2}{2 \omega g^2} \csc^2(\pi \alpha) [2\pi(1 - \alpha) + \sin(2\pi \alpha)] \\ Z_{\perp, q} &= \frac{\pi \alpha^2}{\omega g^2} \csc(\pi \alpha) [1 + \pi(1 - \alpha) \cot(\pi \alpha)] \\ Z_{\perp} &= \frac{\pi \alpha^2}{2 \omega g^2} \csc^2(\pi \alpha / 2) [\pi(1 - \alpha) + \sin(\pi \alpha)], \end{aligned} \quad (30)$$

where $\alpha = g/b$. These curves are plotted in Fig. 9. The round case, with g and b , representing, respectively, the radius of the iris and of the beam pipe, $(Z_{\perp})_{\text{round}} = 2(1/g^2 - g^2/b^4)/\omega$ [8], is also shown (the dashes). We note that Z_{\perp} is always close to and larger for the flat than for the round case.



Collimator Wakes

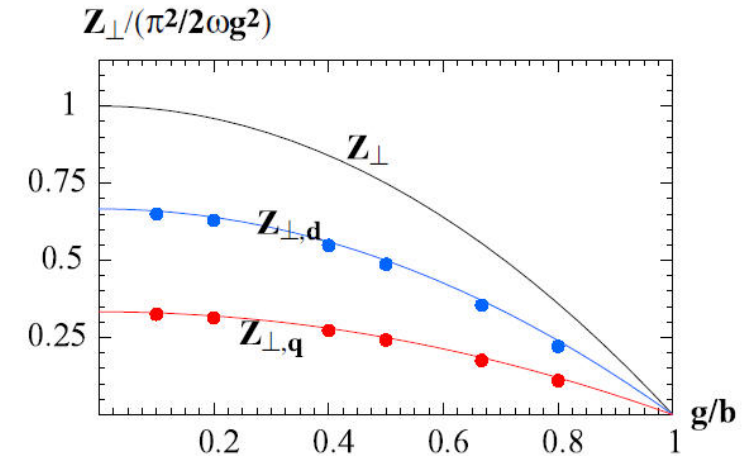
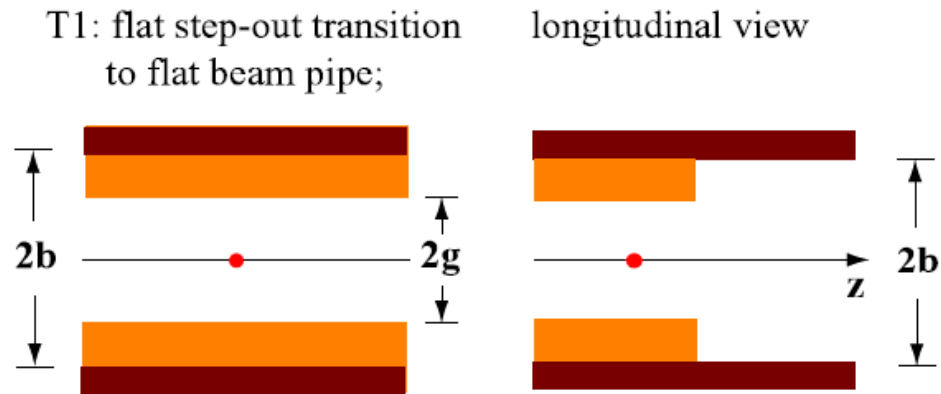


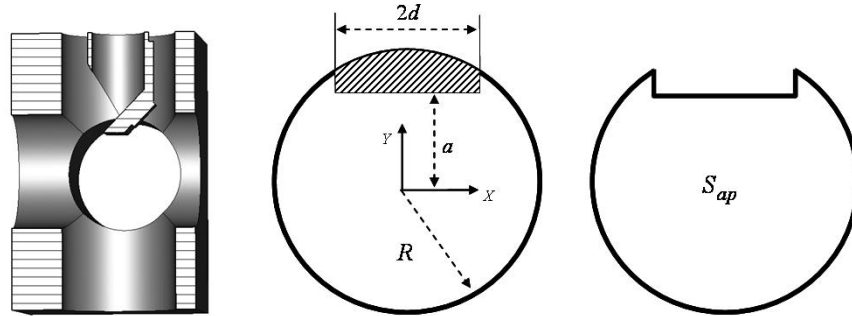
FIG. 13. (Color) For a step-out transition from a flat pipe of aperture $2g$ into a flat pipe of aperture $2b$, the transverse impedances Z_{\perp} , $Z_{\perp,d}$, $Z_{\perp,q}$ as functions of $\alpha = g/b$. Plotting symbols give ECHO numerical results for comparison.

$$Z_{\perp} = \frac{\pi^2}{2\omega} \left(\frac{1}{g^2} - \frac{1}{b^2} \right), \quad (42)$$

with $Z_{\perp,q} = \frac{1}{2} Z_{\perp,d}$. We see thus that the transverse impedance of a flat step-out transition (or of a long, flat collimator) is a factor $\pi^2/8$ times the transverse impedance of a long, round collimator, if we take the half-heights in the former case to be equal to the radii in the latter [6]. In Fig. 13 we plot the theoretical dependence and compare with ECHO numerical results (the plotting symbols). We see that the agreement is very good.

High-Frequency Impedances

TRANSVERSE IMPEDANCE OF LASER MIRROR OF RF GUN



$$\alpha = \tan^{-1} \left(\frac{d}{a} \right)$$

$$\beta = \cot^{-1} \left(\frac{d}{Q} \right) - \tan^{-1} \left(\frac{a}{d} \right)$$

$$Q = \sqrt{R^2 - d^2}$$

$$B = a^2 + d^2$$

$$A = 4\pi^2 \varepsilon_0 \omega a^2 R^4 d^2$$

$$Z_y^{(m)}(\omega) = \frac{1}{2\varepsilon_0 \pi^2 \omega a R^2} \left[(R^2 - 2a^2) \alpha + ad \left(1 + \ln \frac{R^2}{a^2 + d^2} \right) \right]$$

$$Z_y^{(d)}(\omega) = A^{-1} \left[aR^4 d - 4a^3 d^3 + R^4 d^2 \alpha - a^2 \left(2d^3 Q + R^4 \beta + R^2 d (Q - 4d(\alpha + \beta)) \right) \right]$$

$$Z_y^{(q)}(\omega) = \frac{1}{AB} \left[ad \left(R^4 (d^2 - a^2) + (a^2 + d^2) (R^2 + 6d^2) a Q \right) + B \left(a^2 (R^4 - 8d^4) \beta + (R^4 - 8a^4) d^2 \alpha \right) \right]$$

$\sigma = 0.5 \text{ mm}$

$\sigma = 2 \text{ mm}$

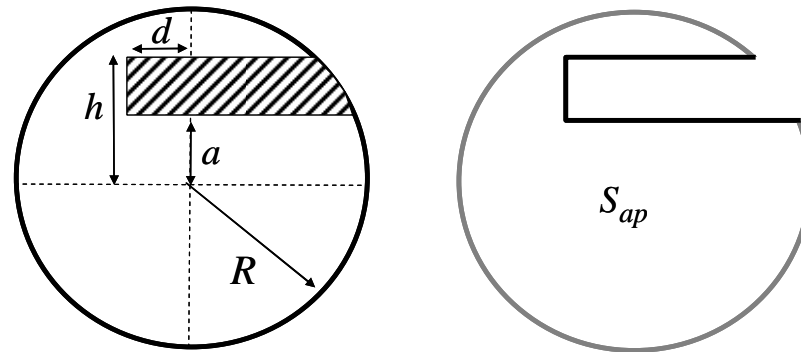
	$k_y(0,0),$ V/pC	$k_y^{(d)},$ V/pC/ m	$k_y^{(q)},$ V/pC/ m
Analytical	0.124	13.1	12.1
Numerical	0.120	13.1	11.6

	$k_y(0,0),$ V/pC	$k_y^{(d)},$ V/pC/ m	$k_y^{(q)},$ V/pC/ m
Analytical	0.12	13	12
Numerical	0.08	24	7.5



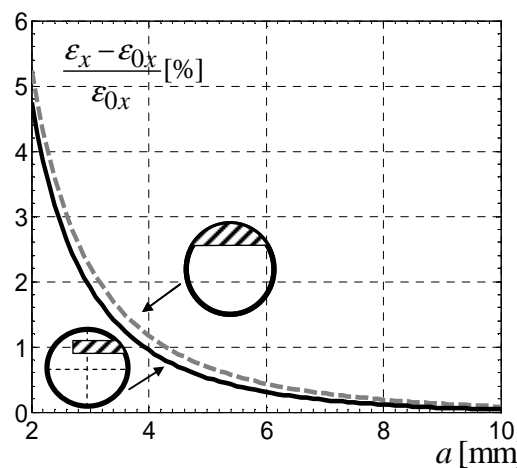
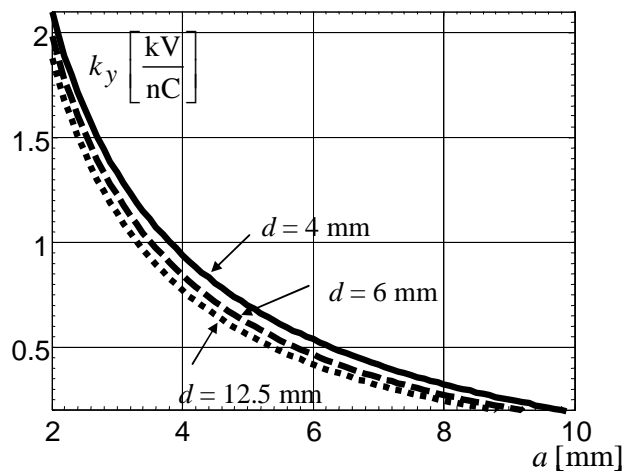
High-Frequency Impedances

TRANSVERSE IMPEDANCE OF OTR SCREENS



$$Z_y^{(m)}(\omega) = \frac{1}{4\pi^2 \epsilon_0 \omega a R^2 h} [F(a, h) - F(h, a)]$$

$$F(x, y) = (R^2 - 2x^2)y \left(\cot^{-1} \left(\frac{x}{\sqrt{R^2 - x^2}} \right) + \tan^{-1} \left(\frac{d}{x} \right) \right) + ay \left(\sqrt{R^2 - x^2} + d \ln(d^2 + y^2) \right)$$

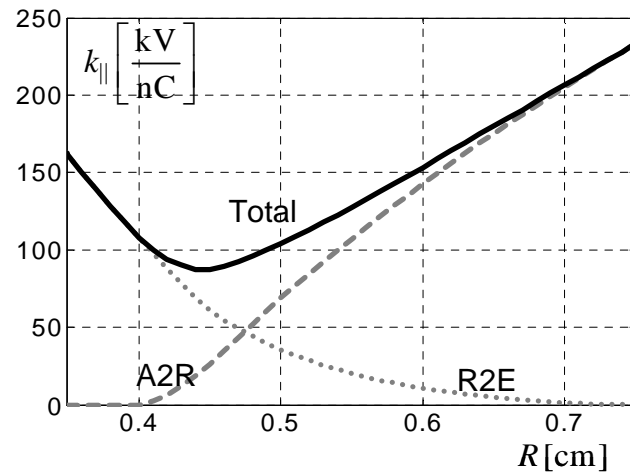
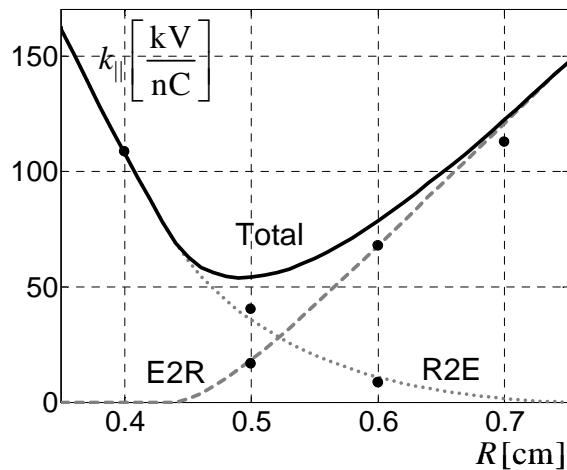
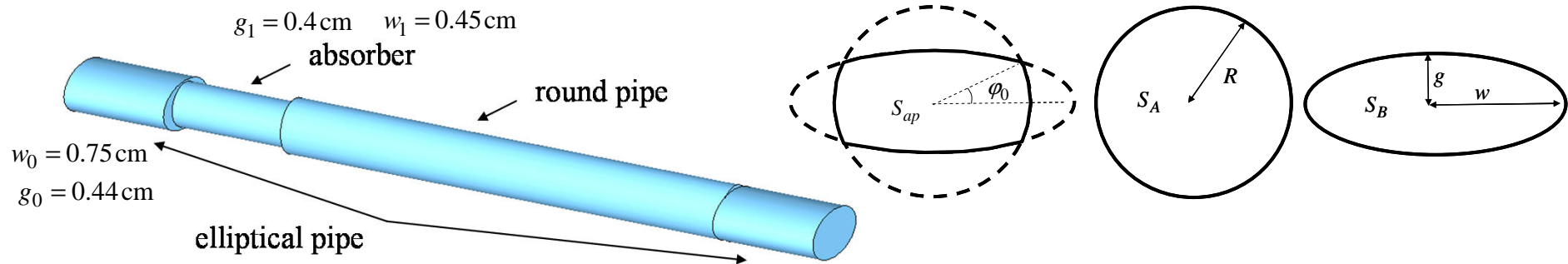


$$\frac{\epsilon_y - \epsilon_{0y}}{\epsilon_{0y}} = \sqrt{1 + S^2 \frac{\beta}{3\epsilon_{0y}}} - 1 \approx S^2 \frac{\beta}{6\epsilon_{0y}}$$

$$S = \frac{eQk_y}{\beta_z^2 E}$$

High-Frequency Impedances

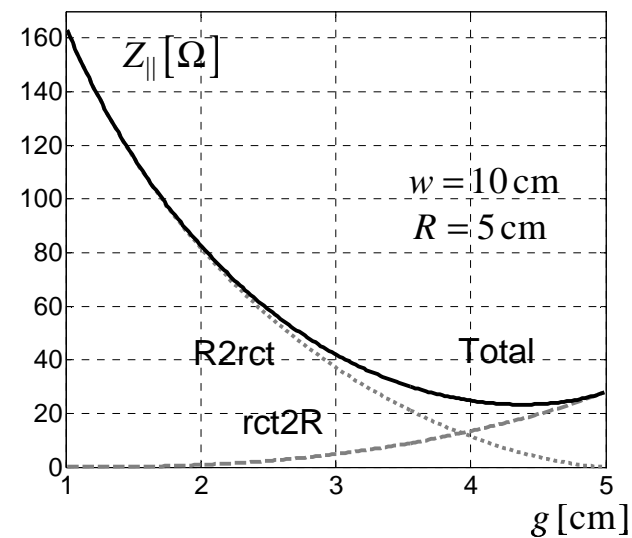
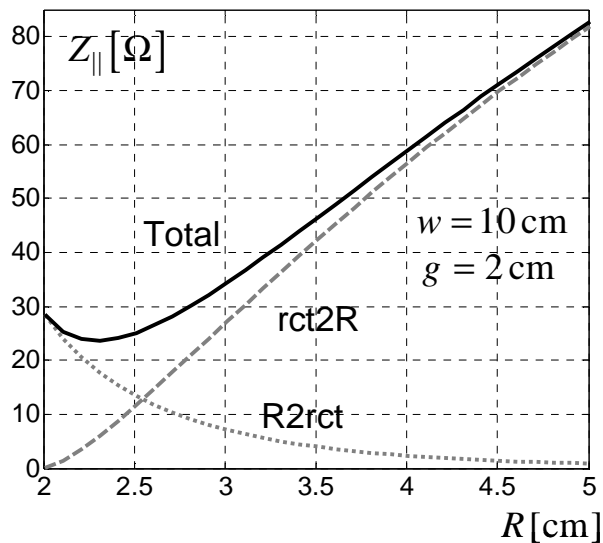
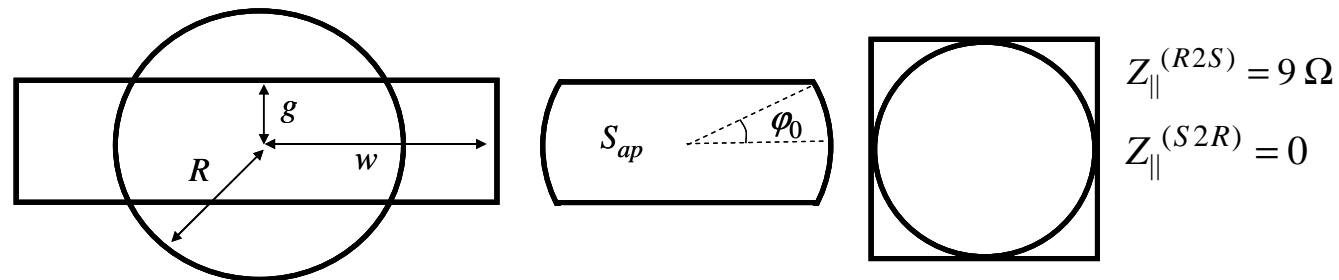
LONGITUDINAL IMPEDANCE OF ELLIPTICAL TO ROUND TRANSITIONS IN UNDULATOR SECTION



Dependence of the loss factor from the radius of the round pipe. The left graph presents the results without the absorber, the right graph presents the results with the absorber included. The black dots show the numerical results from CST Particle Studio.

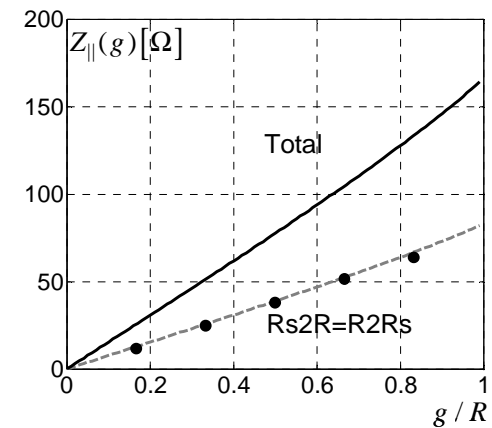
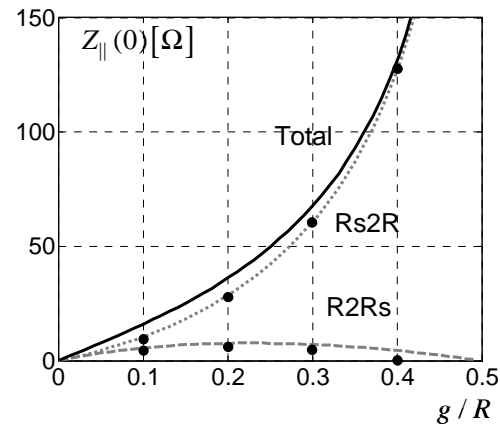
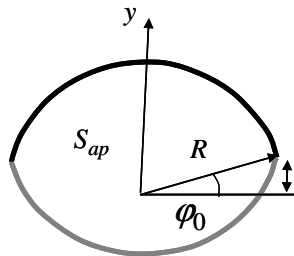
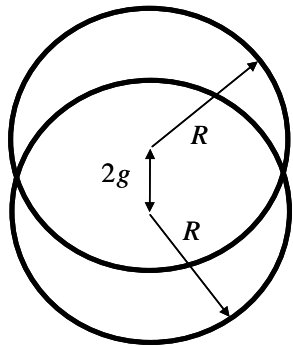
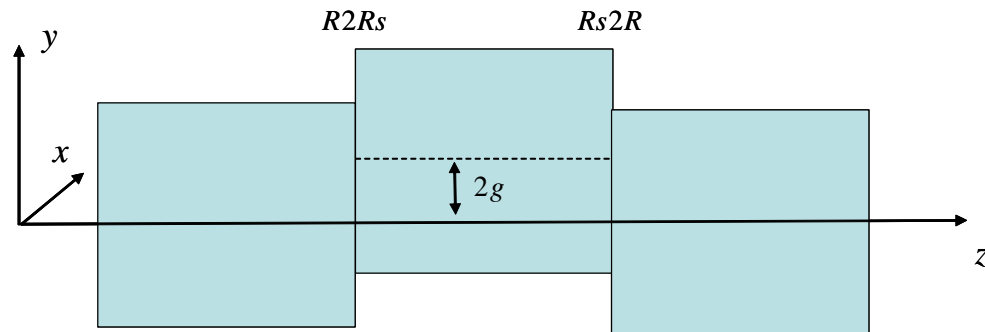
High-Frequency Impedances

LONGITUDINAL IMPEDANCE OF ROUND TO RECTANGULAR TRANSITIONS IN BUNCH COMPRESSORS



High-Frequency Impedances

LONGITUDINAL AND TRANSVERSE IMPEDANCES OF ROUND MISALIGNED PIPES

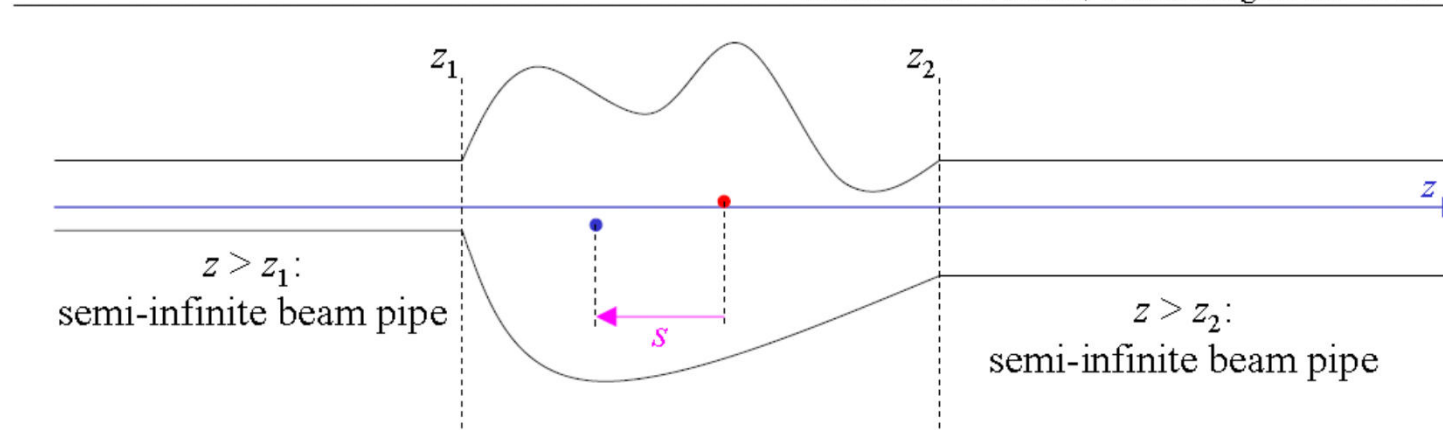


M. Dohlus, I. Zagorodnov, O. Zagorodnova,
High Frequency Impedances in European XFEL, DESY 10-063, 2010

Longitudinal Impedance Budget

wake fields and impedances

much more: Weiland, Wanzenberg DESY M-91-06



source particle q_s : $\mathbf{r}_s(t) = x_s \mathbf{u}_x + y_s \mathbf{u}_y + c(t - t_0) \mathbf{u}_z$

test particle q_t : $\mathbf{r}_t(t) = x_t \mathbf{u}_x + y_t \mathbf{u}_y + (c(t - t_0) - s) \mathbf{u}_z$

wake function: $\mathbf{W}(x_s, y_s, x_t, y_t, s) = \frac{1}{q_s} \int_{-\infty}^{\infty} (\mathbf{E} + \mathbf{v} \times \mathbf{B}) dz \quad \rightarrow \Delta \mathbf{p} = q_s q_t \mathbf{W}$

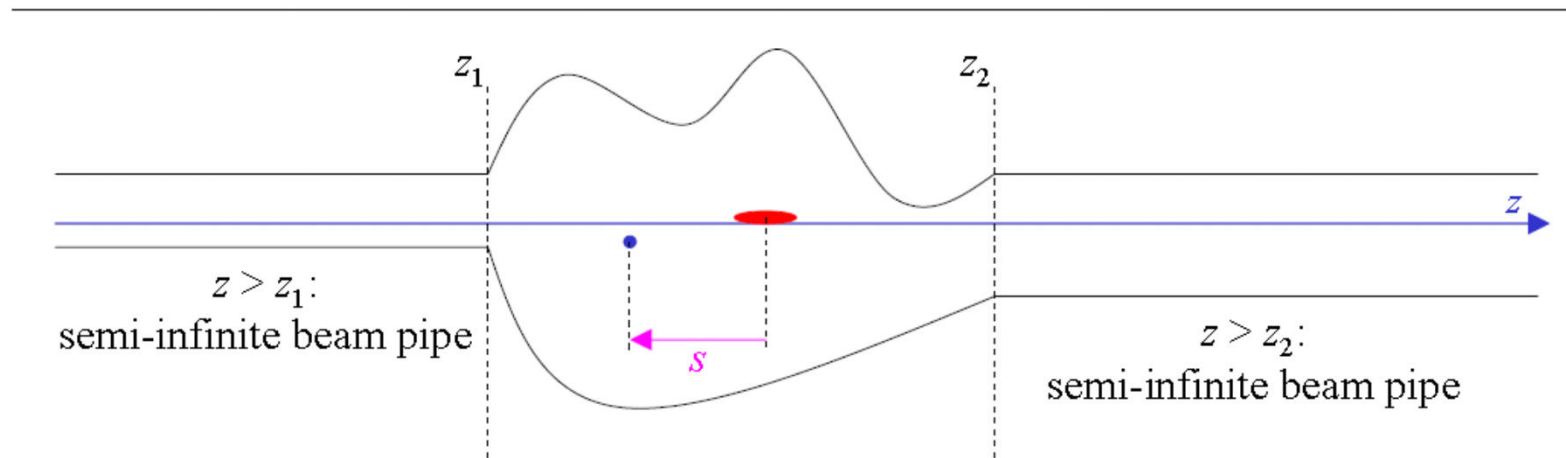
impedance: $Z_{\parallel}(x_s, y_s, x_t, y_t, \omega) = c^{-1} \int_{-\infty}^{\infty} (W_{\parallel}(x_s, y_s, x_t, y_t, s) \exp(-j s \omega / c)) ds$

$Z_{\perp}(x_s, y_s, x_t, y_t, \omega) = -j c^{-1} \int_{-\infty}^{\infty} (W_{\perp}(x_s, y_s, x_t, y_t, s) \exp(-j s \omega / c)) ds$



Longitudinal Impedance Budget

wake potential



source particle \rightarrow source distribution

$$W_{\parallel}(s) = - \int_{-\infty}^s w_{\parallel}(s-s') \lambda(s') ds'$$

wake (Green) function



Longitudinal Impedance Budget

$$W_{\parallel}(s) = - \int_{-\infty}^s w_{\parallel}(s-s') \lambda(s') ds'$$

wake potential \swarrow \nwarrow wake (Green) function

If we know wake function then we can calculate wake potential for any bunch shape. For beam dynamics simulations we need the wake function.

The numerical codes can calculate only wake potentials (usually the Gaussian bunch shape for relatively large rms width is used). But the real bunch shape is far not Gaussian one.

How to obtain the wake function?



Longitudinal Impedance Budget

$$W_{\parallel}(s) = - \int_{-\infty}^s w_{\parallel}(s-s') \lambda(s') ds'$$

wake potential \swarrow \nwarrow wake (Green) function

How to obtain the wake function?

The deconvolution is bad posed operation and does not help.

Well developed analytical estimation for short-range wake functions of different geometries are available.

Hence we can fit our numerical results to an analytical model and define free parameters of the model.

Such approach is used, for example, in

A. **Novokhatsky**, M. **Timm**, and T. **Weiland**, Single bunch energy spread in. the **TESLA** cryomodule, Tech. Rep. **DESY-TESLA-99-16**

T. **Weiland**, I. **Zagorodnov**, The Short-Range Transverse Wake Function for **TESLA** Accelerating Structure, **DESY-TESLA-03-23**



Longitudinal Impedance Budget

- ❑ There are hundreds of wakefield sources in XFEL beam line.
- ❑ The bunch shape changes along the beam line.
- ❑ Hence, a database with wake functions for all element is required.
- ❑ The wake functions are not functions but distributions (generalized functions).
- ❑ How to keep information about such functions?
- ❑ We need a model.



Longitudinal Impedance Budget

Wake function model

$$w(s) = \underbrace{w^{(0)}(s) + \frac{1}{C}}_{\text{regular part}} + \underbrace{Rc\delta(s) - c \frac{\partial}{\partial s} [Lc\delta(s) + w^{(-1)}(s)]}_{\text{singular part (cannot be tabulated directly)}}$$

$$Z(\omega) = Z^{(0)}(\omega) - \frac{1}{i\omega C} + R + i\omega [L + Z^{(-1)}(\omega)]$$

capacitive
resistive
inductive

$$W \sim \int \lambda(s) ds$$

$$W \sim \lambda(s)$$

$$W \sim \lambda'(s)$$

$$\frac{\partial}{\partial s} w^{(-1)}(s) = o(s^{-1}), \quad s \rightarrow 0. \quad \text{it describes singularities } s^{-\alpha}, \alpha < 1$$

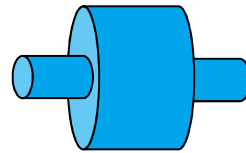


Longitudinal Impedance Budget

$$w(s) = w^{(0)}(s) + \frac{1}{C} + Rc\delta(s) - c \frac{\partial}{\partial s} \left[Lc\delta(s) + w^{(-1)}(s) \right]$$

Pillbox Cavity

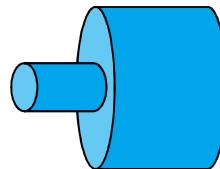
$$w(s) = \frac{Z_0 c}{\sqrt{2\pi^2 a}} \sqrt{\frac{g}{s}}$$



$$w^{(-1)}(s) = -\frac{Z_0}{\sqrt{2\pi^2 a}} \sqrt{sg}$$

Step-out transition

$$w(s) = c \frac{Z_0}{\pi} \ln\left(\frac{b}{a}\right) \delta(s)$$



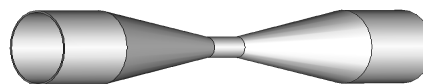
$$R = \frac{Z_0}{\pi} \ln\left(\frac{b}{a}\right)$$

$$w(s) = cR\delta(s)$$

Tapered collimator

$$w(s) = -c^2 \left(\frac{Z_0}{4\pi c} \int r' dr \right) \frac{\partial}{\partial s} \delta(s)$$

$$w(s) = -c^2 L \frac{\partial}{\partial s} \delta(s)$$



$$L = \frac{Z_0}{4\pi c} \int r' dr$$

Longitudinal Impedance Budget

Wake potential for arbitrary bunch shape

$$W(s) = - \int_{-\infty}^s w^{(0)}(s-s') \lambda(s') ds' - \frac{1}{C} \int_{-\infty}^s \lambda(s') ds' - Rc \lambda(s) -$$
$$-c^2 L \lambda'(s) - c \int_{-\infty}^s w^{(-1)}(s-s') \lambda'(s) ds'$$

derivative of the bunch shape



Longitudinal Impedance Budget

The main form of data base application contains a list of element types, parameters R, L, C and links to tables w0 and w_1.

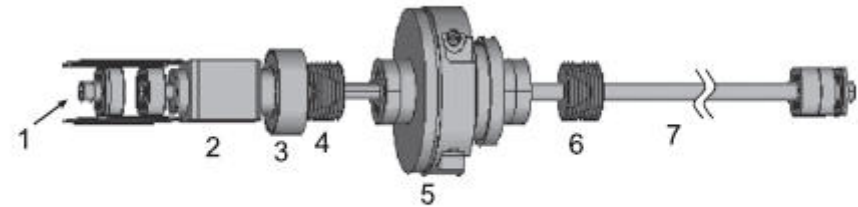


Fig. 6. The European XFEL undulator intersection design. 1—elliptical pipe, 2—pump, 3—absorber, 4,6—bellows, 5—BPM, 7—round pipe.

Wake Field Calculations for the XFEL Project

Search:

Type of element:		<input checked="" type="checkbox"/>	R (Omm):	L (H):	C_inv (1/F):	Link to w0	Link to w_1
ABS	Absorber/Round transition	<input checked="" type="checkbox"/>	2.04E+01	0.00E+00	0.00E+00	AbsRes22mm.dat	0
BEL	Bellow	<input checked="" type="checkbox"/>	7.60E-01	0.00E+00	0.00E+00	BellowRes30mm.dat	BellowDiff1.dat
BPM	BPM	<input checked="" type="checkbox"/>	0.00E+00	0.00E+00	0.00E+00	BPMRes100mm.dat	BPMdiff1.dat
PIPE	Elliptical pipe	<input checked="" type="checkbox"/>	0.00E+00	0.00E+00	0.00E+00	EIPipe5161mm.dat	0
PIPR	Round pipe	<input checked="" type="checkbox"/>	0.00E+00	0.00E+00	0.00E+00	RoundPipe652mm.dat	0
PUM	Pump	<input checked="" type="checkbox"/>	1.13E+00	1.66E-13	0.00E+00	PumpRes105mm.dat	0
RET	Round/Elliptical transition	<input checked="" type="checkbox"/>	1.06E+01	0.00E+00	0.00E+00	0	0
*		<input checked="" type="checkbox"/>	0.00E+00	0.00E+00	0.00E+00		

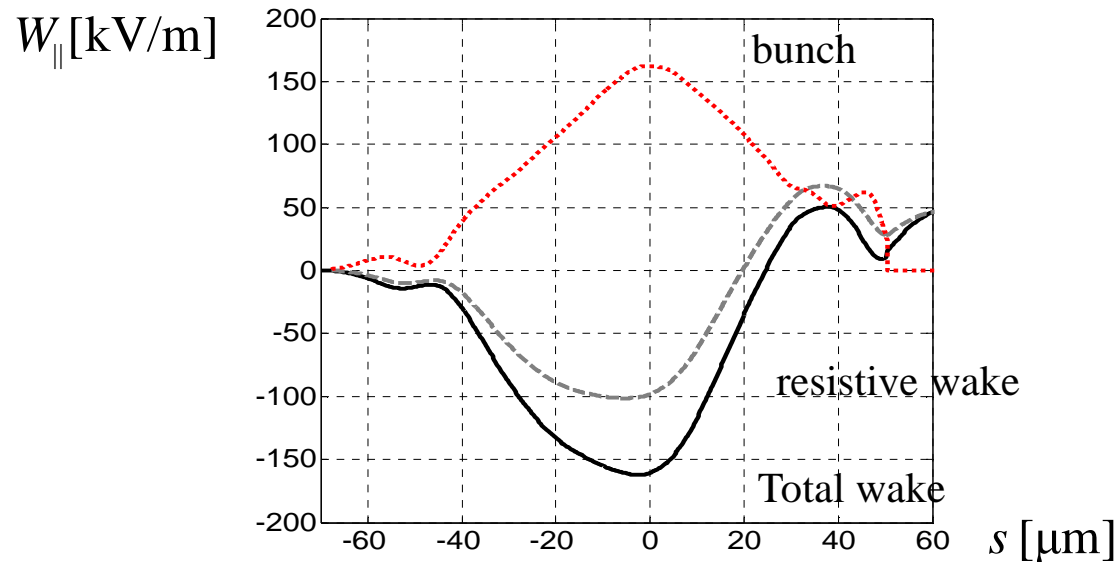
General data Wake Long List ↕

Record: 2 of 7



Longitudinal Impedance Budget

Undulator wake $Q=1nC$



Loss, spread, peak parameters

Section	Type of element	Number	Loss (V/pC)	%	Spread (V/pC/m)	%	Peak (V/pC/m)	%
SA1	ABS	32	2.389E+03	14	8.717E+02	7	3.451E+03	12
SA1	BEL	64	1.342E+03	8	4.476E+02	3	1.803E+03	6
SA1	BPME	33	1.780E+03	11	7.243E+02	6	2.598E+03	9
SA1	PIPE	33	8.730E+03	53	1.020E+04	80	1.844E+04	62
SA1	PIPR	32	7.812E+02	5	1.157E+03	9	2.069E+03	7
SA1	PUM	32	3.025E+02	2	2.383E+02	2	5.476E+02	2
SA1	RET	32	1.228E+03	7	4.422E+02	3	1.766E+03	6
SA1			1.655E+04	100	1.283E+04	100	2.951E+04	100
			1.655E+04	100	1.283E+04	100	2.951E+04	100



Longitudinal Impedance Budget

Undulator wake $Q=1\text{nC}$

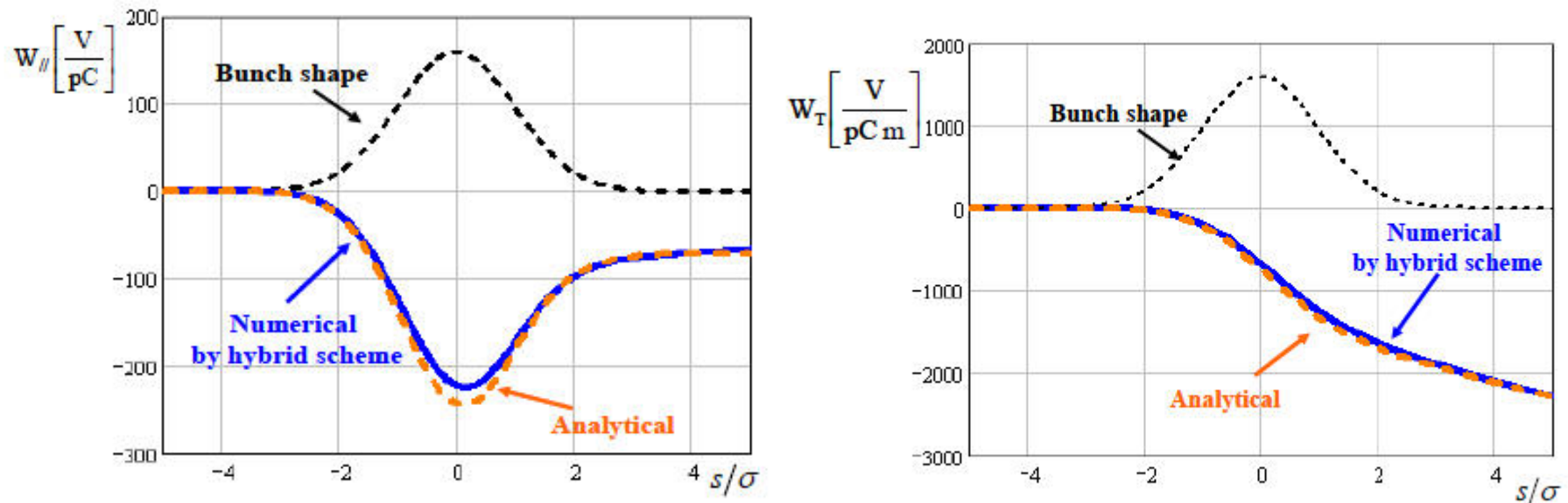


Figure 43. Longitudinal monopole and transverse dipole wake potentials for undulator intersection of European XFEL project calculated by new hybrid numerical scheme (blue solid) and analytically (geom.+resistive) (orange dashed).

TIME DOMAIN NUMERICAL CALCULATIONS OF THE SHORT ELECTRON BUNCH WAKEFIELDS IN RESISTIVE STRUCTURES

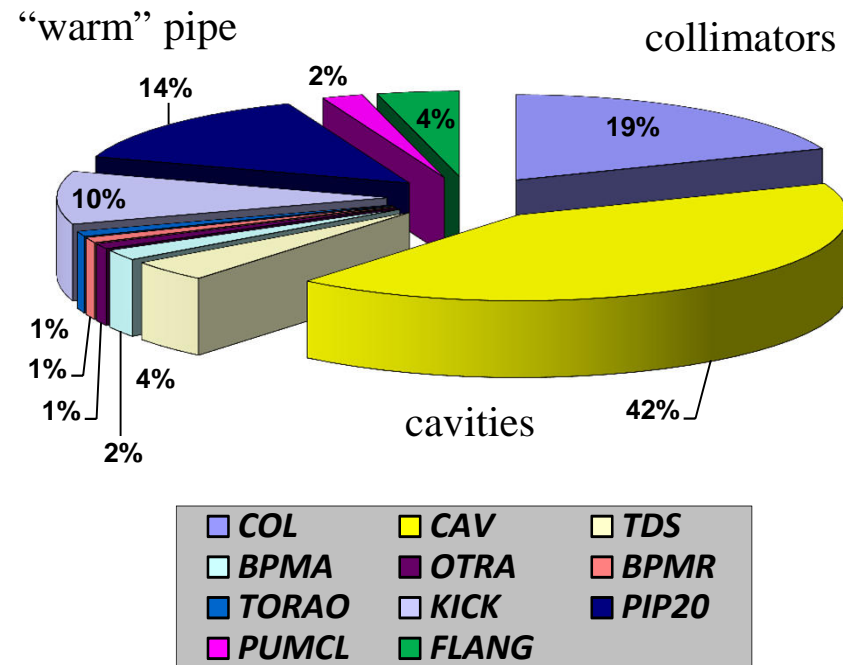
Andranik Tsakanian

Longitudinal Impedance Budget

Accelerator wakes. $Q=1nC$

Impedance Budget (list of elements)

El.type	Num.	Loss (kV/nC)	% Spread	(kV/nC)	% Peak	(kV/nC)	%
BPMF	4	4.075E+01	0	1.858E+01	0	5.804E+01	0
COL	7	6.725E+03	19	3.373E+03	22	1.058E+04	21
KICK	3	3.645E+03	10	1.459E+03	9	5.283E+03	10
PIP20	1	5.116E+03	14	3.661E+03	24	8.959E+03	18
PUMCL	78	5.605E+02	2	2.363E+02	2	7.946E+02	2
CAV	808	1.481E+04	42	8.842E+03	57	2.814E+04	56
CAV3	8	8.084E+01	0	3.010E+01	0	1.117E+02	0
FLANG	500	1.330E+03	4	5.610E+02	4	1.886E+03	4
TDS	8	1.507E+03	4	7.348E+02	5	2.174E+03	4
OTRB	8	1.584E+02	0	7.251E+01	0	2.254E+02	0
STEP1	1	3.010E+00	0	5.969E-01	0	3.441E+00	0
BPMA	107	5.654E+02	2	2.896E+02	2	8.670E+02	2
OTRA	12	3.078E+02	1	1.274E+02	1	4.494E+02	1
BPMC	56	4.431E+01	0	2.138E+01	0	6.805E+01	0
BPMR	26	2.993E+02	1	1.304E+02	1	4.501E+02	1
DCM	4	1.644E+01	0	7.479E+00	0	2.315E+01	0
BPMB	27	5.744E-02	0	1.587E-01	0	6.023E-01	0
BAM	5	3.319E+00	0	1.494E+00	0	4.768E+00	0
TORA	3	3.147E+01	0	1.609E+01	0	4.763E+01	0
TORAO	6	1.856E+02	1	7.684E+01	0	2.700E+02	1
		3.530E+04	100	1.540E+04	100	5.037E+04	100



Longitudinal Impedance Budget

Accelerator wakes. $Q=250$ pC

El.type	Num.	Loss (kV/nC)	%	Spread (kV/nC)	%	Peak (kV/nC)	%
BPMF	4	6.150E+01	0	2.891E+01	0	8.933E+01	0
COL	7	2.283E+04	32	1.022E+04	31	3.452E+04	35
KICK	3	7.893E+03	11	3.100E+03	9	1.052E+04	11
PIP20	1	1.652E+04	23	8.512E+03	26	2.730E+04	27
PUMCL	78	1.103E+03	2	4.743E+02	1	1.574E+03	2
CAV	808	1.574E+04	22	9.440E+03	29	2.987E+04	30
CAV3	8	9.280E+01	0	3.590E+01	0	1.316E+02	0
FLANG	500	2.619E+03	4	1.126E+03	3	3.736E+03	4
TDS	8	2.506E+03	4	1.229E+03	4	3.677E+03	4
OTRB	8	2.428E+02	0	1.137E+02	0	3.510E+02	0
STEP1	1	3.825E+00	0	6.815E-01	0	4.293E+00	0
BPMA	107	7.317E+02	1	4.231E+02	1	1.265E+03	1
OTRA	12	1.698E+02	0	8.118E+01	0	2.474E+02	0
BPMC	56	7.912E+01	0	4.531E+01	0	1.348E+02	0
BPMR	26	1.523E+02	0	7.506E+01	0	2.241E+02	0
DCM	4	2.533E+01	0	1.160E+01	0	3.612E+01	0
BPMB	27	1.247E-01	0	1.976E-01	0	7.440E-01	0
BAM	5	4.474E+00	0	2.180E+00	0	6.820E+00	0
TORA	3	4.681E+01	0	2.515E+01	0	7.275E+01	0
TORAO	6	1.107E+02	0	5.175E+01	0	1.598E+02	0
		7.063E+04	100	3.285E+04	100	1.000E+05	100

